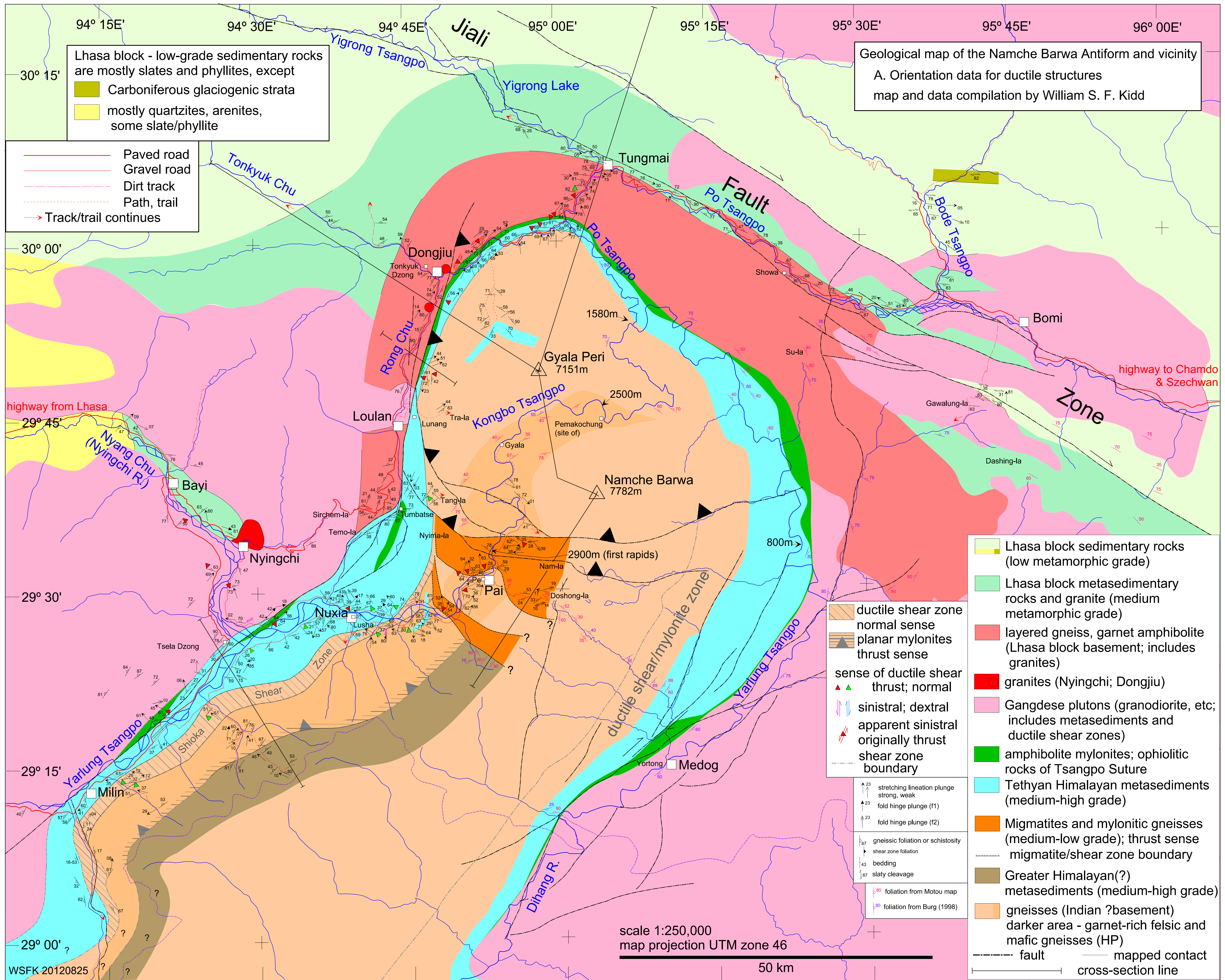


## Figure Captions for Data-Repository Figures

**Figure DR1.** Geological maps of the Namche Barwa antiform and vicinity at 1:250,000 scale. The maps show the same geological units and boundaries as the geological map (text Figure 3) but include significantly more structural field-orientation data and shear- or slip-sense data. (a) The first map in this Data Repository item shows data for ductile structures, including lineation measurements, and shear sense; (b) the second map shows data for brittle structures, including slickenline orientations, and slip sense. These data include those used to construct the stereonet figures (text Figures 6 and 9).

**Figure DR2.** Cartoon cross-sections showing proposed origin of Namche Bara structures. Sections are approximately N to S at the present time; top section through the Gyala Peri (GP) – Namche Barwa (NB) massif; bottom section about 50-75 km west, through the area of the Nyang – Yarlung Tsangpo confluence. Sections are intended to illustrate the idea that shortening localized in the GP-NB crustal-scale fold structure and Nam-la Thrust has been taken from the motion on the Main Himalayan Thrust (MHT). As a result, to the south of the **GP-NB** massif the MHT is less active or inactive, in contrast to the situation farther west. The geomorphology of the foothills of the Himalaya as seen on TM satellite imagery show a contrast from unpedimented, continuous ridges west of the exit of the Dihang (or Siang, or Brahmaputra) River from the foothills, to pedimented, incised, less continuous morphology east of this place, suggesting a reduction or cessation in the activity of the shallow southern part of the MHT, the Main Boundary Thrust (MBT), across this position.



Lhasa block - low-grade sedimentary rocks are mostly slates and phyllites, except  
 Carboniferous glaciogenic strata  
 mostly quartzites, arenites, some slate/phyllite

Geological map of the Namche Barwa Antiform and vicinity  
 A. Orientation data for ductile structures  
 map and data compilation by William S. F. Kidd

Paved road  
 Gravel road  
 Dirt track  
 Path, trail  
 Track/trail continues

Lhasa block sedimentary rocks (low metamorphic grade)  
 Lhasa block metasedimentary rocks and granite (medium metamorphic grade)  
 layered gneiss, garnet amphibolite (Lhasa block basement; includes granites)  
 granites (Nyingchi; Dongjiu)  
 Gangdese plutons (granodiorite, etc; includes metasediments and ductile shear zones)  
 amphibolite mylonites; ophiolitic rocks of Tsangpo Suture  
 Tethyan Himalayan metasediments (medium-high grade)  
 Migmatites and mylonitic gneisses (medium-low grade); thrust sense  
 migmatite/shear zone boundary  
 Greater Himalayan(?) metasediments (medium-high grade)  
 gneisses (Indian ?basement) darker area - garnet-rich felsic and mafic gneisses (HP)  
 fault  
 mapped contact  
 cross-section line

ductile shear zone normal sense  
 planar mylonites thrust sense  
 sense of ductile shear thrust; normal  
 sinistral; dextral  
 apparent sinistral originally thrust  
 shear zone boundary

stretching lineation plunge strong, weak  
 fold hinge plunge (f1)  
 fold hinge plunge (f2)  
 gneissic foliation or schistosity  
 shear zone foliation  
 bedding  
 slaty cleavage  
 foliation from Motou map  
 foliation from Burg (1998)

scale 1:250,000  
 map projection UTM zone 46  
 50 km

Figure DR1b

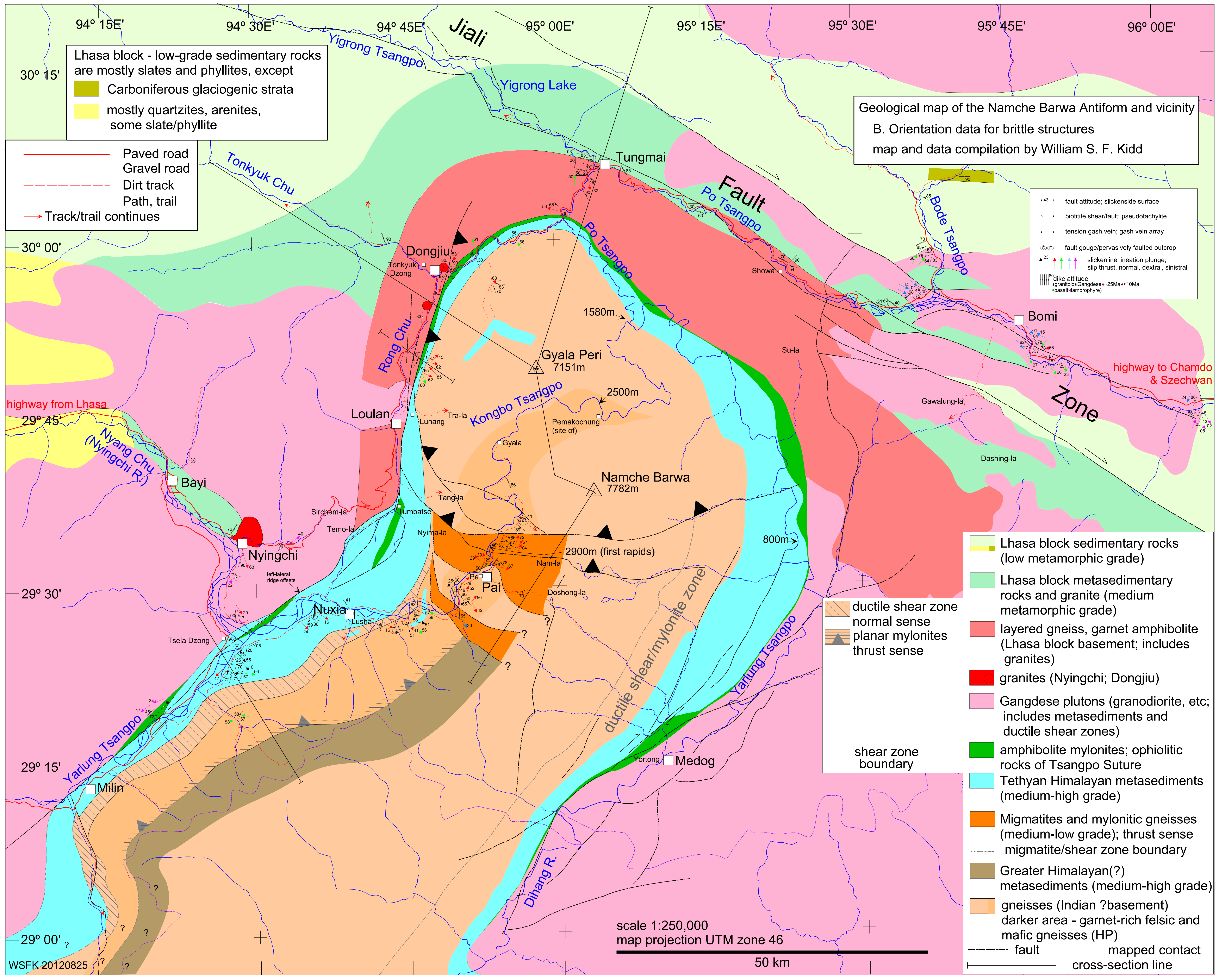
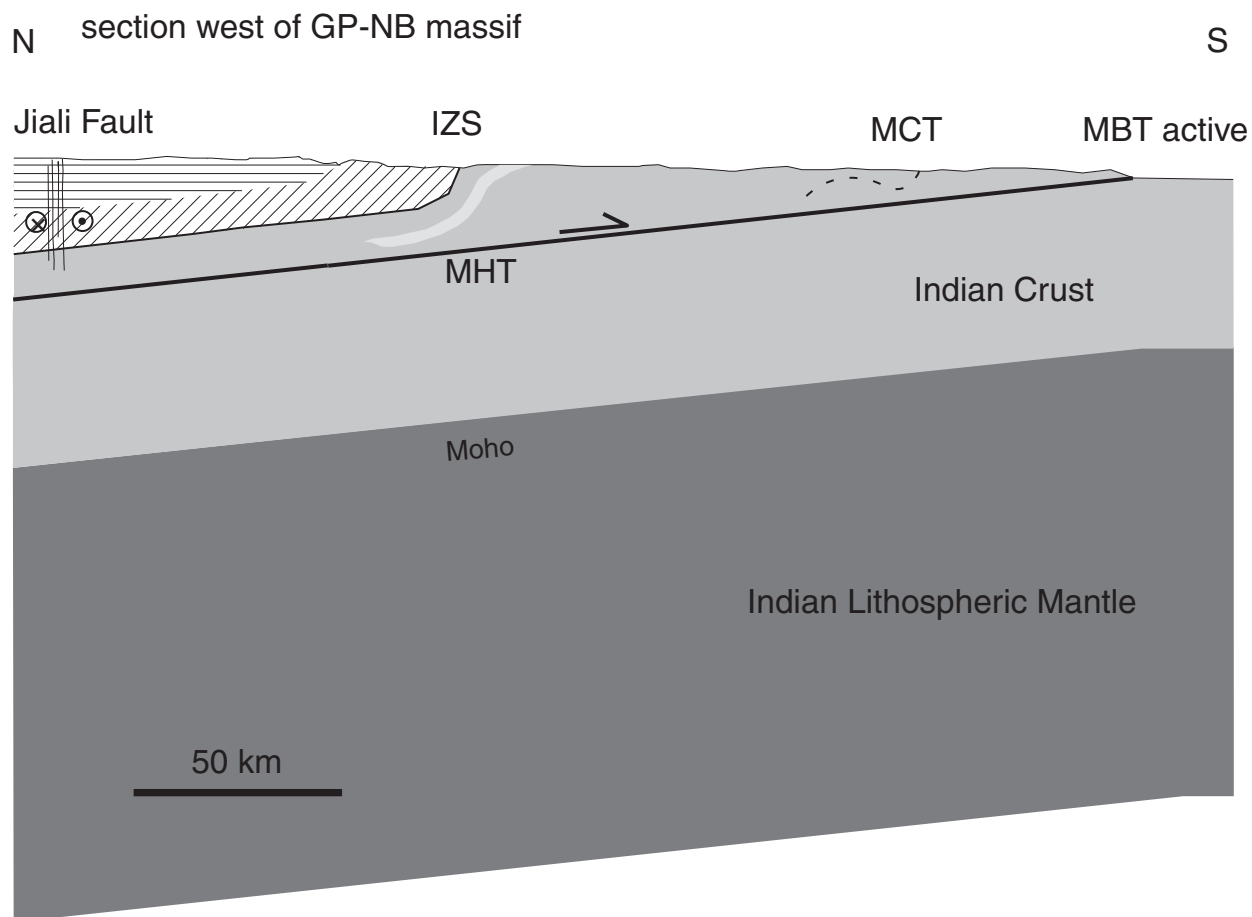
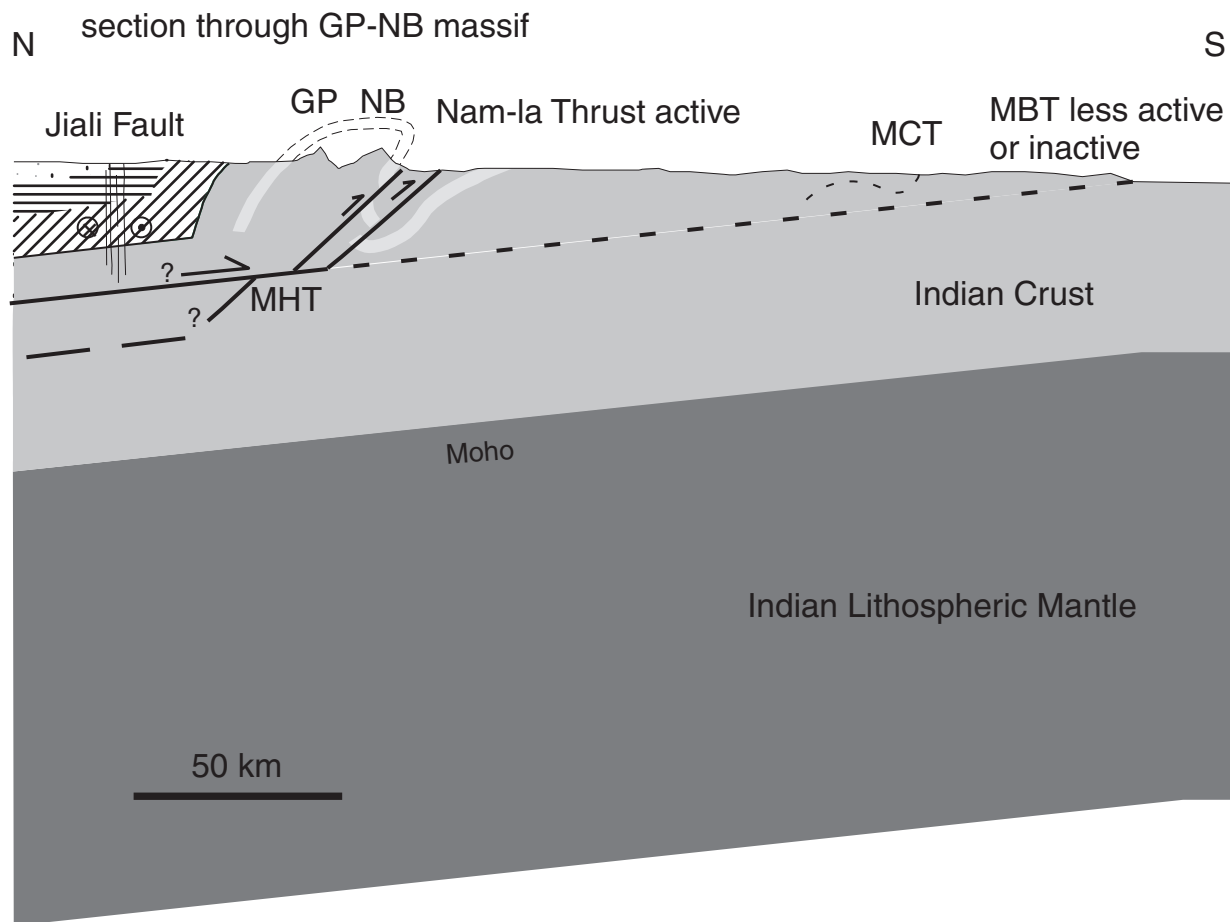


Figure DR2



## REFERENCES CITED IN DATA REPOSITORY ITEMS

- Butera, K.M., Williams, I.S., Blevin, P.L., and Simpson, C.J., 2001, Zircon U-Pb dating of Early Paleozoic monzonitic intrusives from the Goonumbra area, New South Wales: *Australian Journal of Earth Sciences*, v. 48, p. 457-464.
- Compston, W., Williams, I. S. and Mayer, C., 1984, U-Pb geochronology of zircons from lunar breccia 73217 using a sensitive high mass-resolution ion microprobe: *Journal of Geophysical Research*, v. 89, p. B525– B534, doi:10.1029/JB089iS02p0B525.
- Compston, W., Williams, I.S., Kirschvink, J.L., Zhang, Z., and Ma, G., 1992, Zircon U-Pb ages for the Early Cambrian time-scale: *Geological Society of London Journal*, v. 149, p. 171-184 , doi:10.1144/gsjgs.149.2.0171.
- Cumming, G.L., and Richards, J.R., 1975, Ore lead isotope ratios in a continuously changing earth: *Earth and Planetary Science Letters*, v. 28, p. 155–171, doi:10.1016/0012-821X(75)90223-X.
- Farley, K.A., 2002, (U-Th)/He dating: Techniques, calibrations, and applications: *Reviews in Mineralogy and Geochemistry* , v. 47, p. 819–844 doi:10.2138/rmg.2002.47.18.
- Farley, K.A., Wolf, R.A., and Silver, L.T., 1996, The effects of long alpha-stopping distances on (U-Th)/He dates: *Geochimica et Cosmochimica Acta*, v. 60, p. 4223– 4229, doi:10.1016/S0016-7037(96)00193-7.
- Ludwig, K.R., 2001, Squid, version 1.05, A user's manual: Berkeley Geochronology Center Special Publication 2, 17 p.
- McDowell, F., McIntosh, W., and Farley, K., 2005, A precise  $^{40}\text{Ar}$ - $^{39}\text{Ar}$  reference age for the Durango apatite (U-Th)/He and fission-track dating standard: *Chemical Geology*, v. 214, p. 249–263, doi:10.1016/j.chemgeo.2004.10.002.

Richter, F.M., Lovera, O.M., Harrison, T.M., and Copeland, P., 1991, Tibetan tectonics from  $^{40}\text{Ar}/^{39}\text{Ar}$  analysis of a single feldspar sample: *Earth and Planetary Science Letters*, v. 105, p. 266–278, doi:10.1016/0012-821X(91)90136-6.

Rothstein, D.A., and Manning, C.E., 2003, Geothermal gradients in continental magmatic arcs: Constraints from the eastern Peninsular Ranges batholith, Baja California, México, *in* Johnson, S.E., et al., eds., *Tectonic evolution of north- western México and the southwestern USA*: Boulder, Colorado, Geological Society of America Special Paper 374, p. 337– 354, doi:10.1130/0-8137-2374-4.337.

Schmitz, M.D., and Bowring, S.A., 2001, U-Pb zircon and titanite systematics of the Fish Canyon Tuff: an assessment of high-precision U-Pb geochronology and its application to young volcanic rocks: *Geochimica et Cosmochimica Acta*, v. 65, p. 2571–2587, doi:10.1016/S0016-7037(01)00616-0.

Spell, T.L. and McDougall, I., 2003, Characterization and calibration of  $^{40}\text{Ar}/^{39}\text{Ar}$  dating standards: *Chemical Geology*, v. 198(3-4), p. 189–211, doi:10.1016/S0009- 2541(03)00005-6.

Williams, I. S., 1992, Some observations on the use of zircon U–Pb geochronology in the study of granite rocks: *Transactions of the Royal Society of Edinburgh: Earth Sciences*, v. 83, p. 447–458, doi:10.1017/S0263593300008129.

File DR1 nb\_thermochron.kmz

File DR2 nb\_epicenters.kmz

File DR3 nb\_image\_overlays.kmz

File DR4 age data summary

SAMPLE	ELEVATION	LONGITUDE	LATITUDE	He-AP AGE	APerr 2sig	He-ZIR AGE	ZIRerr 2sig	Ar-BIOT AGE	BIOTerr 2sig
CL-03-05	3761	96.15642	30.78993			32.9	2.3		
CL-04-05	3635	95.59628	30.78295			81.1	4.7		
CL-06-05	4208	94.98188	30.7698			46.7	2.7		
BM-06-05	4359	95.75067	30.3507	10.5	0.3	35	1.8		
BM-05-05	4194	95.7495	30.3486	8.24	0.48				
BM-04-05	4059	95.74867	30.34728	7.66	0.24				
BM-02-05	3762	95.74903	30.339	8.53	0.26				
BM-03-05	3922	95.749	30.339	8.05	0.46				
BM-07-05	3498	95.74817	30.3335	7.56	0.36				
NBK-41-23	3207	95.76998	30.24078	8.03	0.26				
BM-01-05	3054	95.76662	30.18522			10.4	0.5		
BT-34-02	2241	94.94405	30.16968			2.05	0.07		
BL-03-03	3432	93.62453	30.13298			13.1	0.7		
BT-35-02	2094	95.0289	30.12792					10.61	0.27
BT-08-03	2062	95.0593	30.0938					15.12	0.15
BT-18-01	2109	95.05958	30.09365			0.35	0.01		
BT-05-03	2070	95.0494	30.07168					43.05	1.5
BT-32-02	2200	95.14352	30.06813					14.86	0.18
BT-02-03	2019	95.03698	30.06422					3.75	0.17
BT-01-03	2027	95.03225	30.05718					4.7	0.07
BT-09-03	2051	95.02858	30.04432					3.22	0.03
BT-01-02	1995	95.01093	30.03883					1.68	0.17
NBK-68-26	3068	94.6315	30.0273			4.08	0.2		
BT-03-02	2069	94.99243	30.01453			0.56	0.02		
BT-24-02	2720	95.30198	30.00088			0.67	0.03	12.87	1.05
BT-05-02	2351	94.90497	29.99998					1.57	0.04
NB02-35	2720	94.72042	29.99603			1.73	0.08		
BT-14-03	2827	94.66807	29.99542					15.94	0.18
BT-36-02	3457	93.10877	29.97305	11.6	0.6				
BT-07-02	2485	94.81162	29.95422	1.68	0.06	1.47	0.04	11.77	0.2
BT-23-02	2600	95.38453	29.95407	0.64	0.02	1.46	0.09	13.73	0.25
b-289	1990	95.08908	29.94585			0.89	0.04	0.23	0.14
NB-60-26	2634	95.38633	29.94492	6.28	0.22				
BT-13-03	2624	94.81287	29.94182					20.39	0.65



BT-16-01	2555	95.40003	29.93765					14.07	0.29
BT-12-03	2686	94.8152	29.93158					16.05	0.52
BT-31-02	2702	95.39213	29.92948			2.89	0.1		
BT-29-02	2750	95.392	29.92927			1.64	0.07		
BT-25-02	2952	95.3834	29.9246	0.74	0.04				
NB-61-26	2653	95.41957	29.92428	2.13	0.06				
GP-14-03	3600	94.88393	29.92348			0.83	0.03		
GP-09-03	3610	94.89592	29.91083			0.71	0.04	0.94	0.03
NB-59-26	2731	95.61668	29.90588	7.35	0.22	5.3	0.16		
NB-63-26	2637	95.49155	29.89152	3.25	0.1	2.26	0.09		
b-279	1530	95.14672	29.89013			0.22	0.01		
b-78	1530	95.14672	29.89013					0.44	0.54
BT-22E-02	2736	95.55458	29.88907	0.41	0.02			15.83	0.25
BC-01-05	2695	95.56852	29.88875	1.35	0.04	7.42	0.52		
NB-55-26	2774	95.76798	29.85388	2.01	0.06				
BT-17-02	3180	94.76647	29.83677			1.92	0.06	16.44	0.24
BT-15-02	3242	94.76973	29.83573					37.99	0.56
BT-12-02	3287	94.7715	29.83477			4.66	0.16	47.18	0.49
BT-20-02	3567	94.78667	29.8276			1.25	0.04	2.19	0.08
BT-19-02	3695	94.79248	29.8236					1.63	0.12
b-188	3290	95.405	29.81417			2.08	0.09	43.44	0.43
BL-02-03	3995	94.42248	29.81105	6.36	0.26				
BR-01-05	4527	94.41437	29.81082	8.52	0.44				
NB-58-26	2852	95.83458	29.81022	2.98	0.1				
BM-02-02	3646	95.69762	29.80927			8.94	0.33	22.45	0.29
NB02-120	4080	94.4212	29.80117	10.1	0.6	13.9	0.3		
NB-56-26	2880	95.76782	29.78498	6.76	0.18				
BC-03-02	2968	95.91572	29.78363			12	1.4	44.08	1.47
BT-12-01	3267	94.74657	29.7819					16.38	0.34
b-265	1470	95.2975	29.77833			0.56	0.03		
BM-05-02	4321	95.68828	29.76892	5.71	0.16				
b-254	3598	95.2085	29.76633			0.5	0.03	1.02	0.05
BM-03-02	4286	95.68518	29.76477			10.2	0.4		
BT-20-01	3110	94.00577	29.76127	18.1	0.8				
b-247	2748	95.15843	29.75812			0.72	0.02	3.43	0.09

b-232	2713	94.9599	29.75467			0.27	0.01	1.66	0.05
b-261	3250	95.22627	29.75228					1.75	0.04
BT-20E-02	3090	94.18418	29.7522	9.07	0.28	13.2	0.4	42.35	1.29
NBK-83b-25	4157	94.7917	29.7486			1.28	0.04	2.83	0.12
b-237	2767	95.06515	29.74237			0.38	0.01	1.77	0.06
NB-57-26	3076	96.03838	29.73673	4.55	0.12				
NB02-159	3380	94.71827	29.73175			5.31	0.16		
BR-03-05	3515	94.39625	29.72232	5.63	0.18				
BT-37-02	4146	92.03957	29.71673			39.3	1.5		
BS-01-05	3087	96.01993	29.70908	2.8	0.08				
BL-01-03	3224	94.3887	29.69012	7.12	0.3	9.92	0.34		
BR-04-05	3154	94.3813	29.6894	8.78	0.24				
BC-03-05	4434	96.72808	29.6787	52.6	1.7	52.9	2.8		
BT-03-05	4677	94.60128	29.64568	8.45	0.36	9.18	0.32		
IG-4	2818	94.92088	29.67435					1.92	0.21
IG-6b-01	2984	94.92678	29.6319			1.15	0.04		
BT-09-01	4179	94.71062	29.63175	3.95	0.2	5.63	0.26	17.14	0.21
BT-01-05	4667	94.59518	29.62802	7.59	0.32				
b-141	1990	95.40058	29.62238			0.57	0.06	25.58	0.28
BC-02-02	3440	96.36503	29.61442			25.9	1.1	107.9	0.53
BT-08-02	3811	94.71748	29.61058	8	0.36	4.45	0.17		
b-143	4100	95.60627	29.60167					17.8	0.29
IG-11-01	4309	94.9906	29.58045					2.12	0.07
BT-04-01	3028	94.46368	29.5789					18.5	0.38
IG-14b-01	3222	94.90813	29.56667					2.45	0.07
BT-02-05	3911	94.57548	29.56632	5.62	0.2	8.56	0.29		
BT-04-05	3523	94.56537	29.56597	5.6	0.24				
b-115	1900	95.41375	29.56375			1.06	0.04		
IG-15a-01	3113	94.89263	29.53975			1.33	0.04	2.45	0.06
BL-09-03	2954	94.42968	29.52708	8.64	0.36	9.39	0.57	18.75	0.22
b-376	1021	95.4542	29.52523					15.57	0.24
BL-18-03	2988	94.45057	29.52033					18.09	0.46
BL-06-03	3877	94.25983	29.50427	6.88	0.38	9.94	0.42		
BL-05-03	4258	94.22167	29.50365	7.41	0.34	8.51	0.34	22.63	0.23
BL-07-03	3738	94.27518	29.50322	6.2	0.26	9.01	0.47		

NB-69-26	3759	94.38987	29.49238	7.86	0.24				
NB-70-26	3660	94.38783	29.49233	8.56	0.24				
BL-08-03	3285	94.3164	29.49118			8.49	0.5		
NB-71-26	3548	94.38608	29.49093	6.91	0.18				
NB-72-26	3453	94.38575	29.49005	7.51	0.22				
BT-21E-02	2940	94.56495	29.48903	4.66	0.22	5.49	0.27	20.92	0.72
NB-73-26	3368	94.385	29.48828	6.51	0.18				
NBK-36-23	2940	94.83077	29.48818	1.79	0.06				
NB-75-26	3198	94.38348	29.48772	7.37	0.24				
NB-74-26	3276	94.38338	29.4877	6.25	0.18				
IG-16-01	4227	94.9466	29.4875			1.48	0.06		
NBK-95-25	2938	94.76442	29.48532					4.4	0.12
IG-19-01	3057	94.83285	29.48073			2.48	0.09	4.12	0.1
B-39	3380	94.9792	29.47518					4.46	0.24
BL-11-03	2977	94.53385	29.4716	5.78	0.18			12.76	3.02
NBK-86-25	3137	94.72773	29.47103					3.64	0.09
IG-20b-01	3097	94.76272	29.46832			2.76	0.11		
NBK-92-95	2937	94.80845	29.46283					3.1	0.08
BT-01-01	2931	94.6493	29.46707			3.52	0.15	4.91	0.11
BL-15-03	3024	94.47737	29.46123					18.25	0.18
NB02-102	2960	94.4266	29.45865			6.92	0.39		
BL-13-03	2951	94.50335	29.45465					6.12	0.19
b-45	905	95.41935	29.45383					35.85	1.01
NBK-15-23	3001	94.69147	29.4393					8.32	0.17
NB02-100	2940	94.44885	29.43513					24.03	0.5
GS149	3250	94.62768	29.39883					5.39	0.08
NB-41-26	3777	94.25458	29.37345	6.88	0.24				
NB-40-26	3703	94.26282	29.37147	5.91	0.18	6.34	0.23		
NB-39-26	3632	94.27095	29.3662	5.8	0.18				
NB-38-26	3607	94.27498	29.36517	5.48	0.16				
NB-37-26	3547	94.28298	29.3639	5.41	0.24				
NB-36-26	3295	94.3073	29.36035	5.77	0.16				
NB-35-26	3251	94.31298	29.3586	6.19	0.26				
NBK-13-23	2964	94.4147	29.3389	4.22	0.14	5.67	0.22		
NBK-14-23	2964	94.4147	29.3389					14.19	0.23

NB-16-26	2974	94.33403	29.325	5.11	0.22				
b-35	1059	95.34522	29.31995			12.1	1.4		
NB-22-26	3016	94.4644	29.31018	3.7	0.12				
b-77	990	95.1765	29.309					20.82	0.69
NB-26-26	3274	94.48345	29.29627	3.8	0.12				
b-138	3760	94.53133	29.25358					5.89	0.1
NBK-55-25	3980	94.5513	29.24953					5.85	0.18
NB-24-26	3629	94.52642	29.24673			5.96	0.25		
NBK-16-23	2974	94.26213	29.24182					8.97	0.49
NB-19-26	3100	94.2907	29.22332	5.31	0.16	5.96	0.24		
NBK-32-25	3363	94.33018	29.19538					8.35	0.24
NB-05-26	2978	94.10278	29.19503	6.94	0.24			89.76	2.7
NB-01-26	2941	94.18373	29.18973	8.11	0.48			9.36	0.17
NB-07-26	3020	94.05457	29.1896	12.5	0.5			57.16	1.76
NB-08-26	3068	93.94445	29.18007	7.16	0.26	8.78	0.34		
NBK-03-23	3223	94.21132	29.17147					9.57	0.198
NB-13-26	3173	94.24797	29.12048	5.17	0.32	5.75	0.26	10.93	0.33
NB-12-26	3132	94.21962	29.08677			6.36	0.32		
NB-10-26	3102	94.22145	29.05965					9.8	0.32
NB-11-26	3163	94.23533	29.04498			6.45	0.33		
SB 13	584	94.92227	29.05752			9.74	1.13		
SB 10	482	94.74808	28.85492			5.34	0.62		
SB 02	464	95.09038	28.46728			7.71	4.68		

Ages in Ma; uncertainties are two-sigma analytical uncertainties in age (Ma).

Samples are currently sorted north to south

## Table DR1

### Methods, Ion-Probe U-Th/Pb Analysis of Zircons

Standard polished grain mounts of separated zircons were analyzed using the SHRIMP RG and SHRIMP II ion microprobes at the Research School of Earth Sciences (RSES), Australian National University in Canberra, following standard procedures (Compston et al., 1984, 1992). U/Pb ratios were referenced to RSES standard FC-1 zircon (1099 Ma,  $^{206}\text{Pb}^*/^{238}\text{U} = 0.1859$ ) and U and Th concentrations were determined relative to RSES standard zircon SL13. Raw data were reduced using versions of the Squid 1 package (Ludwig, 2001). Some analyzed spots yielded U contents of well over 5000 ppm, and U-Pb ages for these spots were corrected for a systematic U-correlated U/Pb bias of -1% per 1000 ppm over 5000 ppm (Butera et al., 2001). For this paper, all reported ages are  $^{206}\text{Pb}/^{238}\text{U}$  ages corrected for common Pb using a Cumming and Richards (1975) model for common Pb the same age as the sample, and using  $^{207}\text{Pb}$  for the common-Pb correction assuming concordance in the  $^{206}\text{Pb}/^{238}\text{U}$  and  $^{207}\text{Pb}/^{235}\text{U}$  systems. Uncertainties are reported in Table DR1 at the one-sigma and include uncertainty in the U-Pb calibration against the standard. Low counts rates on  $^{207}\text{Pb}$  preclude us from making effective use of Pb-Pb ages for most analyses, so we report  $^{206}\text{Pb}/^{238}\text{U}$  ages, but given the complexities in zircon zoning and overprinting described below, it is likely that a few of our older U-Pb data represent mixing between between Precambrian, Pan-African, and Neogene components.

2014215\_Table DR1 final.txt



GP12-16.1	2.2	0.1	BT27-13-1	216.7	3.1
GP12-18.1	2.8	0.1	BT27-14-1	217.8	2.2
GP12-16.4	2.8	0.1	BT27-15-1	215	3.1
GP12-13.1	2.9	0.1	BT27-16-1	198	4.2
GP12-13.3	3.9	0.1	BT27-17-1	212.3	3.1
GP12-13.2	3.9	0.1	BT27-18-1	213.2	4.7
GP12-01.3	4.4	0.1	BT27-20-1	62.5	1.3
GP12-16.3	4.5	0.1	BT27-21-1	173.5	1.7
GP12-10.1	4.6	0.1	BT27-22-1	208.9	2.8
GP12-18.3	4.6	0.1	BT27-23-1	209.4	2.2
GP12-16.5	4.6	0.1	BT27-24-1	211.8	2.6
GP12-22.1	4.7	0.1	BT27-25-1	117.7	1.2
GP12-22.2	5.1	0.1	BT29-1-1	21.8	1.1
GP12-02.2	6.7	0.2	BT29-2-1	23.2	2
GP12-10.2	7.3	0.2	BT29-3-1	307.4	3
GP15(2)-4.1	2.3	0	BT29-4-1	23.6	1.4
GP15(2)-02.1	6.4	0.1	BT29-5-1	24.8	0.7
GP15(2)-03.1	7.1	0.1	BT29-6-1	25.3	1.2
GP15(2)-5.1	9.1	0.2	BT29-7-1	49.2	3.7
GP15(2)-02.2	79.5	1.7	BT29-8-1	34.8	0.9
GP15-11.1	4.2	0.2	BT29-8-2	46.9	1.6
GP15-13.1	4.7	0.2	BT29-9-1	211.3	9.1
GP15-12.1	5.1	0.2	BT29-10-1	165	6.4
GP15-12.2	5.9	0.2	BT29-11-1	23.7	0.9
GP15-9.1	7.5	0.3	BT29-12-1	24.4	0.4
GP15-1.2	8.5	0.3	BT29-13-1	23	1.1
GP15-10.1	8.6	0.3	BT29-14-1	23.6	0.7
GP15-9.2	8.6	0.3	BT29-15-1	23.5	1
GP15-8.1	8.7	0.3	BT29-16-1	25.7	0.5
GP15-5.1	8.7	0.3	BT29-20-1	24.7	0.9
GP15-13.2	9	0.3	BT29-21-1	21.9	1.2
GP15-2.1	9.2	0.3	BT29-23-1	24.4	2
GP15-1.1	9.2	0.3	BT29-24-1	26.7	0.4
GP15-3.1	9.7	0.4	BT29-25-1	23.4	0.8
GP15-6.1	11.6	0.4	BT29-26-1	25.1	1.3
GP15-3.2	68.7	1.8	BT29-27-1	22.2	1.5
GP15-13.3	85.8	3.3	BT29-28-1	22.5	1.6
GP15-9.3	376.6	13.7	BT29-29-1	26.2	0.8
GP15-04.2	2.3	0.1	BT29-30-1	27	1.7
GP15-04.1	2.4	0.1	BT29-31-1	26.2	2.4
GP15-01.1	2.6	0.1	BT29-32-1	146.8	8.9
GP15-02.1	3.9	0.1	BT29-33-1	34.3	0.7
GP15-10.5	4.4	0.1	BT29-34-1	191.7	5.5
GP15-10.6	4.4	0.2	BT31-1-1	38.6	0.8
GP15-10.1	5.1	0.1	BT31-2-1	39.7	1.3
GP15-02.2	6.2	0.2	BT31-3-1	54	2.4
GP15-02.3	6.7	0.2	BT31-4-1	43.6	0.9
GP15-02.4	8.1	0.2	BT31-6-1	51	0.8
GP15-10.2	8.7	0.2	BT31-10-1	46.7	1.5
GP15-10.4	8.9	0.2	BT31-11-1	42.9	0.4
GP15-01.2	9.1	0.2	BT31-12-1	44.8	0.4
GP15-10.3	9.2	0.2	BT31-13-1	30.5	2.5
GP15-05.1	9.2	0.2	BT31-14-1	48.7	0.9
GP15-01.4	9.4	0.2	BT31-15-1	47.4	2.3
GP15-06.1	9.4	0.2	BT31-16-1	46.4	2.9
GP15-02.5	9.6	0.3	BT31-17-1	32.7	1.4
GP15-04.3	9.7	0.2	BT31-18-1	40.2	1.5
GP15-01.3	26.1	0.7	BT31-19-1	44.6	0.7
Booth et al. 2004			BT31-21-1	23.4	0.4
BT19-02-1	19.6	1.3	BT31-22-1	33.7	1.6
BT19-02-2	89.3	3.3	BT31-23-1	37.5	1
BT19-02-3	15.6	1.6	BT31-24-1	51.2	3.2
BT19-02-4	105.6	5.8	BT31-25-1	29.4	0.7
BT19-02-5	169.2	2.4	BT33-1	30.3	0.3
BT19-02-6	19.1	2.6	BT33-2	20.2	0.3
BT19-02-7	14	1.3	BT33-3	20.1	0.3
BT19-02-8	102.2	2.1	BT33-4	20	0.3
BT19-02-9	16	0.9	BT33-5	74	1.1
BT19-02-11	16.5	1.3	BT33-6	74.1	1.4
BT19-02-12	114.8	2.6	BT33-7	30.9	0.3
BT19-02-13	20.8	1.7	BT33-8	25.9	0.3
BT20-02-1	523.6	7.4	BT33-9	21.7	0.3
BT20-02-2	479.4	6.2	BT33-10	21.7	0.3
BT20-02-3	306.8	10.4	BT33-11	33.8	0.4
BT20-02-4	384	5.3	BC01-02-1	118.9	1.4
BT20-02-5	458.6	6.7	BC01-02-2	116.9	1.3
BT20-02-7	490.8	6.5	BC01-02-3	113.3	1.3
BT20-02-8	451.2	8.8	BC01-02-4	832.5	9.6
BT20-02-9	493.1	11.1	BC01-02-5	110	1.6
BT20-02-10	463.8	10.4	BC01-02-6	115.8	1.3
BT20-02-11	510.1	8.9	BC01-02-7	111.2	1.7
BT20-02-12	462.8	7.5	BC01-02-8	119.8	1.4
BT20-02-13	491.5	10.5	BC02-02-1	113.4	1.4
Zeitler et al. this paper			BC02-02-2	107	1.5
b232-09.1	6.8	0.1	BC02-02-3	110.6	1.5
b232-01.1	9.2	1.1	BC02-02-4	119	1.4
b232-09.2	11.7	0.2	BC02-02-5	116.5	1.4
b232-06.1	15.1	0.3	BC02-02-6	111.1	1.4
b232-20.1	18.7	0.3	BC02-02-7	134.4	1.5
b232-05.1	20	0.4	BC03-02-1	117.5	1.5
b232-11.1	21.9	0.4	BC03-02-2	114.8	1.7
b232-03.1	21.2	0.4	BC03-02-3	116.4	1.6
b232-19.1	22.2	0.4	BC03-02-4	116.8	1.6
b232-21.1	23.7	0.5	BC03-02-5	113	1.5
b232-04.1	32.4	0.6	BC03-02-6	116.5	1.7
b232-19.2	416.9	13.2	BM02-02-1	113.2	2.2
b232-03.2	490.5	8.9	BM02-02-2	118.2	2.8
b232-20.2	497.3	8.4	BM02-02-3	115	1.4
b232-11.2	516.8	8.6	BM02-02-4	119.3	2.5
b232-06.2	518.9	9.5	BM02-02-5	114.7	1.7
b232-21.2	652.7	11	BM02-02-6	114.4	1.7
b253-1-1	492.5	16	BM03-1	61.1	1.2
b253-2-1	481.6	4.6	BM03-2	62.7	1.2
b253-3-1	462.9	7.1	BM03-3	63.4	0.9
b253-4-1	470.9	4.8	BM03-4	64.6	1
b253-5-1	472.2	5.3	BM03-5	66.7	0.9
b253-6-1	476.6	4.6	BM03-6	65.6	0.9
b253-7-2	476	6.7	BM03-7	688.3	7.4
b253-8-1	452.5	5.5	BM03-8	68	0.9
b253-9-1	480.1	10.3	Ding et al., 2001		
b253-10-1	471.4	8.7	94T88	22.5	0.8
b253-12-1	497.4	4.8	94T88	21.5	1
b253-13-1	434.2	4.2	94T88	22.9	1.6
b253-14-1	472.4	6.4	94T88	22.8	0.9
b253-16-1	282.5	11.1	94T88	23.2	0.9
b253-17-1	479.9	7.3			
b253-18-1	470.4	11.5			
b253-19-1	465.8	22.5			

b253-20-1	500.5	8.4		
b253-21-1	469.5	5.7		
b253-22-1	499.1	7.2		
b253-24-1	461.3	5.3		
b254-09.1	480	8		
b254-02.1	494.2	8.2		
b254-11.1	494.5	8.2		
b254-06.2	508.3	9.1		
b254-02.2	516.1	8.6		
b254-19.1	519.6	11.5		
b254-09.2	526.7	8.7		
b254-06.1	528.6	8.9		
b261-06.1	269.5	4.9		
b261-02.1	399.6	7.5		
b261-05.1	553.8	16.9		
b261-01.1	1631.9	28.4		
b261-02.2	1648.5	27.7		
b261-07.1	1692.2	28.9		
b261-04.1	1702	30.1		
b261-05.2	1744.5	33.4		
Booth et al. 2004				
IG19-1-1	531.5	16.1		
IG19-1-2	749.6	15.6		
IG19-2-1	9.8	3.7		
IG19-2-2	744.5	65.2		
IG19-3-1	535.4	5.1		
IG19-3-2	644.4	91.5		
IG19-4-1	245.7	6.7		
IG19-4-2	592.1	33.6		
IG19-5-1	232.5	76.3		
IG19-5-2	1088.5	49.5		
IG19-6-1	482.7	21.6		
IG19-6-2	1032.8	9.5		
IG19-7-1	947.2	32.5		
IG19-8-1	533.4	5.3		
IG19-8-2	1186.3	10.8		
IG19-10-1	2207.9	18.7		
IG19-11-1	733.9	29.9		
IG19-11-2	985	37.3		
IG19-12-1	7.5	1.3		
IG19-12-2	8	2.8		
IG19-13-1	497	11.9		
IG19-14-1	1163.4	35.1		
IG19-15-1	482	26		
IG19-16-1	545.7	13.7		
IG19-17-1	8.9	1.3		
IG19-17-2	8	1.2		
IG19-17-3	264.7	18.2		
IG19-17-4	6.4	1.7		
IG19-18-1	577	5.5		
IG19-19-1	111.5	1.4		
IG19-19-2	474	5.7		
IG19-20-1	1049.2	88.4		
IG19-21-1	536.7	16.8		
IG4-1	3	0.1		
IG4-2	2.7	0.1		
IG4-3	3.9	0.1		
IG4-4	3.6	0.1		
IG4-5	2.8	0.1		
IG8-1	6.4	0.1		
IG8-2	5.9	0.1		
IG8-3	6	0.2		
IG8-4	5.8	0.1		
IG8-5	6.4	0.2		
IG18-1	144.4	1.6		
IG18-2	2.8	0.1		
IG18-3	3.1	0.1		
IG18-4	2.8	0.1		
IG18-5	498.6	2.3		
IG18-6	510.7	2		
IG18-7	2.9	0.1		
IG18-8	481.2	2.4		
IG18-9	3	0.1		
IG18-core1	517.2	9.1		
IG18-core2	528.9	9.4		
IG18-core3	582.7	10.2		
IG18-core4	542.6	9.6		
IG18-core5	529	9.3		
IG18-core6	505.8	9.1		
IG18-core7	511	9		
IG6B-1	9.5	0.2		
IG6B-2	13.4	0.4		
IG6B-3	9.8	0.3		
IG6B-4	9.3	0.3		
IG6B-5	9.7	0.3		
IG6B-6	9.9	0.2		
IG6B-7	10	0.3		
IG6B-8	9.8	0.4	346	6 Nyingchi Complex Guo et al.
IG6B-9	10	0.3	525	4
IG6B-10	854.6	3.7	1069	12
IG6B-11	454.3	2.2	1356	11
IG6B-12	859.4	4	1494	17
IG6B-13	775.6	3.3	413	4
IG6B-14	841.7	4.2	1429	13
IG6B-15	867	4.4	1739	13
IG6B-16	844.9	4.7	2840	20
IG6B-17	9.3	0.3	1135	11
IG2D-1	13.7	0.2	345	4
IG2D-2	21.9	0.4	1629	11
IG2D-3	13.9	0.3	474	4
IG2D-4	30.6	0.4	357	3
IG2D-5	16.4	0.4	888	13
IG2D-6	14.7	0.3	1117	14
IG2D-7	17.1	0.3	1070	8
IG2D-8	18	0.5	342	5
IG2D-core	103.5	1.4	1338	9
IG16-1	3.9	0.3	1448	10
IG16-2	4.2	0.3	956	9
IG16-3	3.1	0.1	962	12
IG16-4	4.6	0.3	440	3
IG16-core1	489.1	5.1	1093	9
IG16-core2	487.4	5.1	1328	10
IG16-core3	498.4	5.2	1478	11
IG16-core4	487.6	5.1	1281	12
IG15A-1	5.9	0.3	1105	10
IG15A-2	6.6	0.2	1170	11
IG15A-3	6.3	0.2	589	5
IG15A-4	6.4	0.3	808	8



IG15A-5	6.3	0.3	926	12
IG15A-6	6.4	0.2	1019	16
IG15A-7	6.1	0.3	1350	13
IG15A-8	6.6	0.1	1566	13
IG15A-9	7.6	0.1	626	5
Ding Lin et al. (2001)			490	5
95T150	293	9	738	6
95T150	64.1	2.2	1069	8
95T150	86.4	3.1	1165	8
95T150	184	5	362	2
95T150	65.1	4.1	843	8
95T150	91	4	333	3
95T150	125	5	339	3
95T150	49.2	6.7	1715	11
95T150	44	1.4	1076	9
95T150	42.6	1	1491	12
95T150	42	3.2	1800	12
95T150	38.3	1.3	2258	13
95T148	19	2	1050	9
95T148	21	2	63.7	0.5
95T148	12	12	63.4	0.6
95T148	13	1	63.4	0.7
95T148	15	1	63.8	0.9
95T148	15	1	63	0.8
95T148	25	1	62.8	0.8
95T148	11	1	62.2	0.7
95T148	17	1	65.4	0.9
95T148	15	1	63.7	0.8
95T148	96	1	38.6	1
95T148	512	3	63.7	0.7
95T148	160	6	61.1	0.6
95T148	162	6	60.6	0.8
95T148	156	4	62.9	1.4
95T148	380	5	54.8	1.5
95T19	485	7	62.7	1.6
95T19	463	9	65.7	2.6
95T19	271	5	65.6	1.1
95T19	13	1	63.9	1.3
95T19	13	1	45.5	0.5
95T19	301	5	85.6	1.2
95T19	135	9	84	1
95T19	357	7	62.2	0.7
95T19	462	16	83.7	0.7
95T19	446	6	56.5	1.1
95T19	17	1	55.8	0.6
95T19	79	3	84.7	1.3
Zhang et al. 2012 NB gneisses			84.8	1
	465	2	64.5	2
	480.4	0.3	83.1	1.1
	484.6	0.2	64	0.9
	491.9	1.8	84.1	2.2
	492.8	2.5	84.6	1.2
	493.4	2.7	80.2	0.6
	493.7	1.2	88.5	1.5
	494.5	2.2	62.6	2.7
	495	0.4	64.7	1.1
	496.8	0.3	64.5	2.3
	498.6	12.5	83.5	3.1
	507.6	3.3	51.4	0.6
	467	4	56	1.3
	473	4	82.4	1.3
	476	4	63.3	0.6
	486	4	78.2	1.5
	488	4	84.9	1.8
	488	4	86.3	2
	488	4	64.1	2.5
	490	4	82.6	1.2
	490	4	1579	19.6
	492	4	461	13.8
	496	4	1019	25.1
	496	4	65.2	1.3
	496	4	64.2	1.2
	497	4	569	7.9
	497	4	65.1	0.8
	498	4	610	7.9
	498	4	648	10.6
	499	4	922	12.7
	500	4	403	4.8
	503	4	1448	15
	511	4	55.2	1
	512	5	560	14.7
	514	4	67.8	1
	516	6	55.9	1.1
	522	4	1524	21.9
	16	0.2	999	12.3
	24.4	0.3	65.9	2.7
	27.8	0.3	1370	26.9
	28.8	0.3	52.5	0.9
	300	3	494	6.4
	349	3	431	11.1
	361	3	908	12.9
	424	4	756	15.7
	444	4	2658	31.8
	458	4	1125	13.8
	466	4	982	12.5
	471	4	1052	11.6
	482	4	1017	18.9
	480	4	1123	15.8
	480	4	299	4
	482	4	553	6.4
	483	4	511	7.1
	482	4	376	5.1
	486	4	64.4	0.6
	493	4	40.7	0.6
	491	4	347	11.7
	499	4	63.5	0.7
	500	4	391	11.1
	503	4	63.8	0.6
	503	4	56.2	0.8
	504	4	42.4	0.7
	506	4	63.8	1.9
	501	4	54.6	1
	513	4	55.7	1.2
	512	4	1018	15.5
	512	4	55.8	1.2
	532	4	41.3	0.9
	516	5	419	17.8
	534	5	64	0.7

20.1	0.3	63.7	0.7
20.7	0.3	64.6	0.8
21	0.3	26.1	0.4 Xu et al. 2012 marginal ("DWSZ" - suture)
18.9	0.4	25	1.1
22.6	0.4	25.7	0.5
19	0.4	26	0.9
25.9	0.4	24.1	1
32.7	0.4	26.3	1
297	2	27.4	2.1
424	3	25.7	0.8
444	3	26.4	1.3
458	3	24.4	1
471	4	23.7	0.9
477	3	24	0.8
480	4	53.8	1.5
487	4	55.2	1.3
495	4	55	1.5
498	4	50.1	1.5
500	4	52.9	1.3
495	4	53.9	1
500	4	50.1	2.9
499	4	55.5	2.7
516	4	53.8	5.5
504	4	57.1	3.2
501	4	54.4	5.3
508	4	57	1.5
513	4	52.7	2.6
514	4	53.4	2.4
518	4	31.2	0.9
514	4	32.6	1.1
527	4	30.8	0.6
559	5	30.9	0.4
1546.8	7.8	31.2	0.3
1549.8	13.5	31.8	0.9
1566.1	12.5	31.8	0.6
1568.4	6.6	31.3	0.8
1579.2	8.6	30.8	1.3
1608.4	7.3	31.1	0.9
1634.2	9.5	30.9	0.6
1638.2	7.3	33.3	0.8
1661.7	8.7	22.9	0.7
1664.2	12.9	23.1	0.6
1666.8	6.6	22.3	0.7
1340.8	13	22.3	0.9
1425.1	12.6	21.9	0.6
1447.8	12	23	0.7
1500	11.7	23.2	0.6
1519.7	14.9	22.9	0.6
1530.9	11.9	23.8	0.6
1535.2	11.6	22.6	0.5
1538.7	12.3	23.3	0.5
1541.9	13.3	24.9	0.6
1542.4	17.9	24.1	0.5
1559.1	13		
1561.2	12		
1561.6	13.1		
1574.1	11.1		
1593.9	12.4		
1598.2	17.4		
1633	12.7		
1865.7	14		
1869.5	14.6		
1874.8	14.5		
1597	6.5		
1611.1	5.6		
1636.9	8.7		
1650.8	7.3		
1652	6.4		
1665.3	7.1		
1671.5	9		
1672.6	7.1		
1676.3	9.7		
1680.9	9.5		
1697.3	8.6		
1719.8	11.3		
1721.7	7.9		
1744.6	10		
474	4		
481	4		
486	4		
494	4		
509	4		
744	7		
941	7		
968	7		
1574	11		
1581	11		
1523	10		
1617	11		
1629	11		
1609	11		
1650	12		
1670	12		
1635	12		
1656	12		
1660	12		
1665	12		
1698	12		
1642	11		
1698	12		
1805	12		
1858	13		
2474	16		
12.5	0.3		
14.7	0.2		
17	0.3		
18.9	0.5		
19.4	0.5		
19.4	0.3		
20.3	0.4		
20.7	0.4		
20.9	0.4		
21.7	1.2		
27	0.5		
28.9	0.8		
36.1	1.6		
77.5	1.2		
201.1	2.4		

716.7	3.9
780.2	6.2
789.7	4.3
798.2	5.1
823.2	9
833	6
892.4	4.9
897.1	5.9
991.4	6.1
1001.6	12.8
1027.4	7.1
1029.5	6.4
1056.6	6.7
1181.4	7.5
1213.3	9.5
1235.9	17.1
1288.8	7
1330.8	7.1
1526.3	12.5
1598.3	10.5
753.5	24.7
1131.9	13.7
1463.9	10.5
1515.9	11.9
1564.4	12.5
1565.6	10.8
1572	16.4
1594.3	16.1
1597.6	10.8
1598	12.5
1607	12.5
1608.5	12
1612.6	15.1
1616	17.1
1630	14.8
1634.7	19.3
1646.7	18.2
1682.2	13.3
1704.2	12
1754	19.9
1759.8	15.5
1810.8	17
1823.6	12.6
1832.9	14.2
2297.1	16.3
8.1	0.2
8.2	0.2
8.2	0.2
8.4	0.3
8.8	0.3
313	3
453	5
459	5
459	5
462	5
466	5
468	5
471	5
478	5
483	5
486	5
492	5
493	5
496	5
497	5
498	5
499	5
504	5
504	5
505	5
505	5
505	5
505	5
506	5
507	5
508	5
508	5
508	5
509	5
510	5
511	5
512	5
517	5
520	5
540	6
544	6

Zeng et al. 2012 NB gneisses

16.5	0.3
20.5	0.5
21.3	0.4
21.7	0.4
22.1	0.4
22.7	0.4
23.8	0.4
24.2	0.5
24.8	0.5
24.8	0.4
25.1	0.5
44.1	1
170.4	2.8
377.1	6.2
577	10
785	24
826	13
928	14
1075	18
1217	19
1266	19
1759	64
24.1	0.3
24.2	0.3
24.2	0.3
24.4	0.3
24.4	0.3
25	0.5
25	0.5
25.2	0.3
25.3	0.4

	25.3	0.3
Xu et al. 2010 NB gneisses - "DMSZ" samples not included	10.8	0.3
	10.2	0.3
	9.8	0.3
	10.9	0.3
	9.8	0.3
	10	0.3
	10.6	0.3
	9.6	0.4
	9.5	0.3
	10.4	0.3
	9.6	0.3
	9.9	0.3
	10.1	0.2
	893.9	18.8
	384.1	9.5
	24.3	0.6
	23.4	0.5
	23.9	0.5
	22.8	0.4
	22.5	0.4
	23.1	0.5
	23.7	0.5
	22.6	0.5
	23.6	0.5
	22.4	0.4
	23.9	0.5
	22.8	0.5
	24.6	0.6
	23.1	0.4
	22.5	0.4
	23.4	0.4
	23.5	0.4
	23.4	0.4
	23.9	0.4
	5.2	0.4
	4.5	0.5
	4.6	0.2
	5.4	0.3
	6	0.5
	4.3	0.2
	5.7	0.3
	4.6	0.5
	4.5	0.3
	4.4	0.3
Xu et al., 2010 NB gneisses	5.9	0.4
	19.3	0.4
	23.3	0.7
	30	2
	18.8	0.4
	24.4	0.8
	23.2	0.7
	24.6	0.8
	24.7	0.8
	24.8	0.6
	23.4	0.9
	28.2	1
	24.8	0.9
	25	1
	23.9	0.8
	24.3	0.8
	18.6	0.4
	23.4	0.8
	24.4	0.9
	18.5	0.4
	23	0.6
	23.2	0.7
	24	1
	23.9	0.7
	18.9	0.4
	24.3	0.8
	24.4	0.8
	18.5	0.4
	25	1
	24.1	0.8
	19.1	0.4
	25	1
	19.1	0.5
	17	1
	17.1	0.8
	18	0.6
	16.9	0.9
	17	1
	17	2
	17.6	0.8
	16	2
	17.3	0.8
	17	1
	16.6	0.7
	16.9	0.8
	17.3	0.6
	18	1
	16.4	0.8
	15.7	0.8
	16.9	0.8
	17	1
	16	1
	17.1	0.8
	16.2	0.7
	16	2
	24.3	0.6
	493	8
	24.6	0.5
	490	8
	490	8
	489	8
	493	8
	24.4	0.6
	490	9
	491	8
	488	8
	492	8
	24.6	0.7
	804	12
	492	8
	486	8

490	8
24	1
490	8
487	8
24.3	0.8
1101	17
24.6	0.6
23	0.7
492	8
492	8
24.2	0.6
495	7
488	7
487	7
495	7
482	7
23	1
489	7
17	0.5
479	7
531	5
802	8
1028	11
664	7
1010	10
1062	11
1020	14
1093	11
1007	10
2040	22
1029	12
1078	11
480	5
495	5
1803	18
610	7
665	7
833	9
890	10
651	7
586	7
1374	15
1346	15
823	9
906	10
1004	12
1177	13
24	0.7
829	9
771	10
495	6
1626	19
672	9
924	13
818	10
789	10
924	12
Su et al. 2012 NB gneisses	
23.7	0.4
23.1	0.4
24.1	0.4
25.1	0.4
24.7	0.4
25.2	0.5
25.2	0.4
25.7	0.4
26.7	0.4
26.7	0.5
464.9	7.5
481.5	10.1
496	7.5
504.5	8
498.8	7.6
502.6	7.7
503.7	7.3
505.4	7.3
521.2	7.6
521.7	7.6
557.6	8
583.7	9.7
17.5	0.3
17.7	0.3
17.8	0.3
18	0.3
18.3	0.3
18.3	0.3
18.4	0.3
18.4	0.3
18.6	0.4
18.7	0.3
18.7	0.4
18.8	0.3
18.8	0.3
20.8	0.3
23.2	0.4
22.5	0.4
23.4	0.5
24.4	0.4
25.2	0.4
1805.8	23.8

This table list information about ALL samples collected for the Indentor Corners project.

Most samples are archived at Lehigh University; what aliquots or whole-rocks remain depend on if, how, and for what purpose the sample was analyzed.

**LEGEND FOR SAMPLE DESIGNATORS**

Lehigh sample numbers are in form DD-##-YR

Kidd designators are in form NBKYR-## or NBYR-##

IG -- Inner Gorge: Along Tsangpo, from confluence with Nyang River and downstream

BT -- Bayi to Tungmai to Bomi. Overused designator that for some years extends from west of Bayi along Nyang River, along main road to Chengdu, all the way past Tungmai to Bomi. Includes some Gyala Peri massif sample as well (i.e., Deu Gungbu section).

NB, NBK -- samples taken by Bill Kidd, across whole region

BC -- Bomi to Chamdo along main road to Chengdu then on to Chamdo

BM -- Bomi to Medoc (from Bomi, south up to pass to Medoc)

BX -- From Lhasa - Bayi road, north to Xoka and to east.

BL -- Bayi -- Lhinze area, both sides of Nyang River and above

GP -- Transect into Gyala Peri from Parlung at north, down Layo Valley

DX -- A single sample (!) west of Dongjiou

CL -- Chamdo to Lhorong, 2005 Spring field season

NCH, TJ -- several samples ESE of Naqu, headwaters of Salween and Mekong

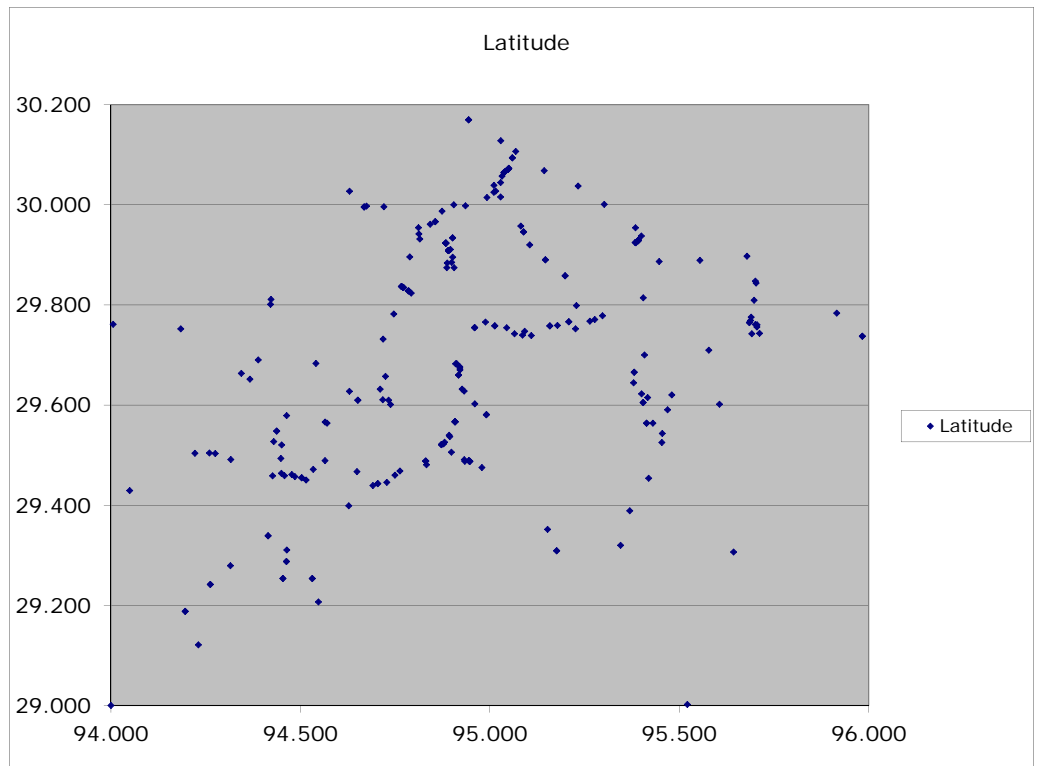
MI, M(00), b-, unadorned number: samples obtained from Chengdu Institute from traverses across inner Namche Barwa massif

Sample	Lat. (deg)	Long. (deg)	Elevatio (m)	Rock Type	Notes	
<b>2001 SEPTEMBER - OCTOBER FIELD SEASON</b>						
<i>GPS locations based on WGS84 datum, almost all 10 m accuracy or better; elevations are barometric with some GPS auto-recalibrati</i>						
<b>"Upper" inner gorge of Tsango, Pai to Jiala traverse</b>						
IG-1-01	29	40.945	94	54.582	2808	strike -N, vertical
	(a)					??
	(b)					qtz vein-xcutting
	(c)					kyanite?-biot gneiss
	(d)					felsic lens biot gneiss
	(e)					garnet-biot gneiss
	(f)					qtz-fldspr pod (concord.)
	(g)					qtz vein (concord.)
IG-2-01	29	40.958	94	54.755	2815	100 section gar amphib -N striking, 80 E
	(a)					garnet amphibolite
	(b)					qtz vein ~concordant
	(c)					mica-rich lense, fault zone
	(d)					deformed felsic melt pod
IG-3-01	29	40.598	94	55.240	2832	3 granitoids, marked as 1
IG-4-01	29	40.461	94	55.253	2818	Leucocratic pegmatite dike
IG-5-01	29	40.217	94	55.273	2821	gar-biot gneiss w/ augen
IG-6-01	29	37.914	94	55.607	2984	strike 325 steep to E strike 90 vertical dip
	(a)					qtz from pod context unclear
	(b)					20 cm felsic dikelet
	(c)					granitic gneiss
IG-7-01	29	37.675	94	55.935	2904	gar biot gneiss
IG-8-01	no GPS lock				3080	1st gully north of Zhibei 1st waterfall above Zhibei
	(a)					odd, altered leucocratic gneiss
	(b)					FLOAT garnet granitoid -- abundant large boulders (shows gradual migmatitic contact with biot gneiss)
	(c)					quartz vein, concordant
<b>Ascend to base camp; PZ crumps; samples collected on walk to WSW towards higher camps by Anne, Zhang, Geng, and</b>						
IG-9-01	29	34.867	94	59.476	4348	(basement) in waterfall
IG-10-01	29	34.827	94	59.436	4309	aplite? 30 m from waterfall
IG-11-01						biotite gneiss at Camp 1 (see map)
IG-12-01	29	36.147	94	57.622		biotite gneiss near Base Camp
<b>Along road, return from Gega to Pai</b>						
IG-14-01	29	34.000	94	54.488		
	(a)					biotite gneiss chlorite on joints
	(b)					qtz vein/pod 3m X 20 cm
IG-15-01	29	32.385	94	53.558	3113	from just E of Pai
	(a)					granitic sweat
	(b)					amphibolite lens
	(c)					biotite gneiss/selvage
<b>Walk up to Doxiong La from end of road</b>						
end jeep road	29	29.527	94	55.652	3763	
Doxiong La	29	29.269	94	56.846	4238	
IG-16-01	29	29.250	94	56.796	4227	KF-bearing banded migm. gorgeous granitic migm.
IG-17-01	29	29.303	94	56.693	4174	biot gneiss and qtz vein

Sample	Lat. (deg)	(min)	Long. (deg)	(min)	Elevatiior (m)	Rock Type	Notes
IG-18-01	29	29.454	94	55.950	3931	FLOAT granite fr. 4m boulder	clearly fr. hdwall above
<b>West of Pai along road</b>							
IG-19-01	29	28.844	94	49.971	3057	biot gneiss outcrop brittle frac	
IG-20-01	29	28.099	94	45.763	3097	biot gneiss altered rox	outcrop faulted
<b>Drive from Bayi past Lhinze along north bank, T-Po</b>							
BT-1-01	29	28.024	94	38.958	2931	biot selvage, white micas	mylonite zone lots faults
BT-2-01	29	27.296	94	30.201	2939	gar-amphib gneiss	
BT-3-01	29	27.532	94	27.482	2976	foliated granite w/ xenoliths	~3variants, plus gar peg
BT-4-01	29	34.734	94	27.821	3028	fresh med-grained granite	just N of Lhinze 25 Ma
BT-5-01	29	39.102	94	22.006	3018	fractured granitoid outcrop	just S of Bayi
<b>Drive from Bayi past Lhinze to Lulan(g) (and also due S of Lulan(g))</b>							
BT-6-01	29	33.967	94	33.911	3522	granite, slightly weathered	see silt units at this elev.
BT-7-01	29	33.832	94	34.226	3810	granite	
BT-8-01	29	36.586	94	39.103	4512	sl. fol. granite, some musc peg	just W of pass
pass (on road)	29	36.644	94	39.129	4559		
BT-9-01	29	37.905	94	42.637	4179	somewhat weathered granitoid	numerous peg. lenses
BT-10-01	29	36.066	94	44.277	3737	augen amphib gneiss	~SE strike vertical dip
BT-11-01	29	36.587	94	43.970	3686	fine-grained amphibolite gneiss	?serpentine in outcrop
<b>Drive from Lulan(g) past Pailong, Tungmai to Bomi</b>							
BT-12-01	29	46.914	94	44.794	3267	fresh granite	
BT-13-01	29	53.754	94	47.325	2743	peg. granite gn. w. amphib encl	
BT-14-01	29	57.980	94	51.343	2460	fine biot gneiss actin. sulfides	
<b>Return (escape from) Bomi to Bayi</b>							
BT-15-01	29	53.838	95	40.726	2685	Bomi (grano)diorite	mild foliation
BT-16-01	29	56.259	95	24.002	2555	highly foliated granitoid	
BT-17-01	30	02.246	95	13.987		qtz peg xcuts amphib +calc sch	
BT-18-01	30	05.619	95	03.575	2109	peg xcutting amphibolite	S of Tungmai
BT-19-01	30	01.636	95	00.931	2070	mica schists two samples	at start of Po-TsangPo
P-TPo bridge	30	01.333	95	00.372	2096	suspension bridge leading to Po-TsangPo access and trek	
<b>Return drive from Bayi to Lhasa via paved "northern" route</b>							
BT-20-01	29	45.676	94	00.346	3110	granite, massive undeformed	
<b>2002 MAY - JUNE FIELD SEASON</b>							
<b>Lulang - Tungmai Road, with Bill Kidd and Chul Lim</b>							
BT-1-02	30	02.330	95	00.656	1995	biot-gar gneiss strained	150m downstrm of Pailong village
BT-2-02	30	01.498	95	00.644			
	(a)					phlogopite-bearing marble	
	(b)					biotite selvage	
	(c)					qtzite w/ white micac selvage	
BT-3-02	30	00.872	94	59.546	2069		
	(a)					qtz vein	
	(b)					amphibolite (and leech!)	
	(c)					biotite gneiss	
BT-4-02	29	59.875	94	56.145	2251		
	(a)					amphibolite lens	
	(b)					biotite gneiss	
BT-5-02	29	59.999	94	54.298	2351	mylonite w/ fresh biotite	
BT-6-02	29	59.234	94	52.429	2405	strained biotite gneiss	
BT-7-02	29	57.253	94	48.697	2485	garnet granite (large sample)	
<b>Walk to pass SSE of end of Lulang Valley (no outcrop!!)</b>							
BT-8-02	29	36.635	94	43.049	3811	qtzofeldspathic gneiss	
<b>Walk up cobble stream across western margin of G-P</b>							
BT-9-02	29	50.086	94	46.290	3376	FLOAT gneissic granite	
BT-10-02	29	50.086	94	46.290	3376	FLOAT gneissic granite	
BT-11-02	29	50.086	94	46.290	3364	garnet amphibolite NO GPS	
BT-12-02	29	50.086	94	46.290	3287	biotite gneiss NO GPS	
BT-13-02	29	50.086	94	46.290	3287	foliated granite NO GPS	
BT-14-02	29	50.086	94	46.290	3259	granitic gneiss	
BT-15-02	29	50.144	94	46.184	3242	granite pegmatite 'thin dike'	
BT-16-02	29	50.144	94	46.184	3242	country rock to BT-15-02	
BT-17-02	29	50.206	94	45.988	3180	granite dike	
BT-18-02	29	50.206	94	45.988	3180	country rock to BT-17-02	
BT-19-02	29	49.416	94	47.549	3695	foliated muscovite granite	
BT-20-02	29	49.656	94	47.200	3567	S/C mylonite	
BT-21-02	29	49.687	94	47.099	3538		
	(a)					pelitic schist	
	(b)					sandier unit	
	(c)					qtz vein-concordant stringer	
BT-22-02	29	49.687	94	47.099	3528	30m to W of BT-21-02; same	
<b>Drive to NW and NNW of Bayi for scouting, granite sampling (lake with temple)</b>							
BX-1-02	30	00.434	93	54.833	3531	biotite from shear zone	
BX-2-02	30	00.377	93	54.677	3549	muscovite gneiss w/ biot phase	
BX-3-02	29	59.758	93	53.630	3513	qtzite w/ white mica	
BX-4-02	29	59.237	93	51.999	3481	qtzite w/ white mica	
BT-19E-02	29	48.662	93	46.832	3221	Gamma 3-5 granitoid	
BT-20E-02	29	45.132	94	11.051	3090	Gamma 6 granitoid	
<b>Drive to northern Bank of Tsangpo to hunt for outcrop towards Lulang (none up high!)</b>							
BT-21E-02	29	29.342	94	33.897	2940	Amphibolite? and biot? gneiss	
<b>Drive towards Medoc from Bomi, towards pass</b>							
BM-1-02	29	46.534	95	41.390	3846	veined epidotized gneiss; aplite?	
BM-2-02	29	48.556	95	41.857	3646	granodiorite	
BM-3-02	29	45.886	95	41.111	4286	granite pegmatite (NH)	

Names and Coords only

Sample	Latitude	Longitude	Latitude
IG-1-01	29.682	94.910	29.682
IG-2-01	29.683	94.913	29.683
IG-3-01	29.677	94.921	29.677
IG-4-01	29.674	94.921	29.674
IG-5-01	29.670	94.921	29.670
IG-6-01	29.632	94.927	29.632
IG-7-01	29.628	94.932	29.628
IG-9-01	29.581	94.991	29.581
IG-10-01	29.580	94.991	29.580
IG-12-01	29.602	94.960	29.602
IG-14-01	29.567	94.908	29.567
IG-15-01	29.540	94.893	29.540
IG-16-01	29.488	94.947	29.488
IG-17-01	29.488	94.945	29.488
IG-18-01	29.491	94.933	29.491
IG-19-01	29.481	94.833	29.481
IG-20-01	29.468	94.763	29.468
BT-1-01	29.467	94.649	29.467
BT-2-01	29.455	94.503	29.455
BT-3-01	29.459	94.458	29.459
BT-4-01	29.579	94.464	29.579
BT-5-01	29.652	94.367	29.652
BT-6-01	29.566	94.565	29.566
BT-7-01	29.564	94.570	29.564
BT-8-01	29.610	94.652	29.610
BT-9-01	29.632	94.711	29.632
BT-10-01	29.601	94.738	29.601
BT-11-01	29.610	94.733	29.610
BT-12-01	29.782	94.747	29.782
BT-13-01	29.896	94.789	29.896
BT-14-01	29.966	94.856	29.966
BT-15-01	29.897	95.679	29.897
BT-16-01	29.938	95.400	29.938
BT-17-01	30.037	95.233	30.037
BT-18-01	30.094	95.060	30.094
BT-19-01	30.027	95.016	30.027
BT-20-01	29.761	94.006	29.761
BT-1-02	30.039	95.011	30.039
BT-2-02	30.025	95.011	30.025
BT-3-02	30.015	94.992	30.015
BT-4-02	29.998	94.936	29.998
BT-5-02	30.000	94.905	30.000
BT-6-02	29.987	94.874	29.987
BT-7-02	29.954	94.812	29.954
BT-8-02	29.611	94.717	29.611
BT-9-02	29.835	94.772	29.835
BT-10-02	29.835	94.772	29.835
BT-11-02	29.835	94.772	29.835
BT-12-02	29.835	94.772	29.835
BT-13-02	29.835	94.772	29.835
BT-14-02	29.835	94.772	29.835
BT-15-02	29.836	94.770	29.836
BT-16-02	29.836	94.770	29.836
BT-17-02	29.837	94.766	29.837
BT-18-02	29.837	94.766	29.837
BT-19-02	29.824	94.792	29.824
BT-20-02	29.828	94.787	29.828
BT-21-02	29.828	94.785	29.828
BT-22-02	29.828	94.785	29.828
BX-1-02	30.007	93.914	30.007
BX-2-02	30.006	93.911	30.006
BX-3-02	29.996	93.894	29.996
BX-4-02	29.987	93.867	29.987
BT-19E-02	29.811	93.781	29.811
BT-20E-02	29.752	94.184	29.752
BT-21E-02	29.489	94.565	29.489
BM-1-02	29.776	95.690	29.776
BM-2-02	29.809	95.698	29.809
BM-3-02	29.765	95.685	29.765
BM-4-02	29.765	95.685	29.765
BM-5-02	29.769	95.688	29.769
BC-1-02	29.508	96.604	29.508
BC-2-02	29.614	96.365	29.614
BC-3-02	29.784	95.916	29.784
BT-22E-02	29.889	95.555	29.889
BT-23-02	29.954	95.385	29.954
BT-24-02	30.001	95.302	30.001
BT-25-02	29.925	95.383	29.925
BT-26-02	29.924	95.385	29.924
BT-27-02	29.928	95.391	29.928
BT-28-02	29.928	95.392	29.928
BT-29-02	29.929	95.392	29.929
BT-30-02	29.929	95.392	29.929
BT-31-02	29.929	95.392	29.929
NB02-35	29.996	94.720	29.996
NB02-159	29.732	94.718	29.732
NB02-102	29.459	94.427	29.459
NB02-103F	29.548	94.437	29.548
NB02-103C	29.548	94.437	29.548
BT-32-02	30.068	95.144	30.068
BT-33-02	30.170	94.944	30.170
BT-34-02	30.170	94.944	30.170
BT-35-02	30.128	95.029	30.128
BT-36-02	29.973	93.109	29.973
BT-37-02	29.717	92.040	29.717
NB02-120	29.801	94.421	29.801
NB02-67	30.071	95.048	30.071
NB02-113	29.663	94.344	29.663
NB02-151A	30.107	95.069	30.107
MIII(00)b-	29.564	95.430	29.564
MIII(00)b-	29.615	95.417	29.615
MIII(00)b-	29.564	95.414	29.564
MIII(00)b-	29.564	95.414	29.564
MIII(00)b-	29.605	95.405	29.605
MIII(00)b-	29.605	95.405	29.605
MIII(00)b-	29.622	95.401	29.622
MIII(00)b-	29.644	95.380	29.644
MIII(00)b-	29.666	95.381	29.666
MIII(00)b-	29.666	95.381	29.666
MIII(00)b-	29.700	95.408	29.700
MIII(01)b-	29.755	94.960	29.755
MIII(01)b-	29.755	94.960	29.755
MIII(01)b-	29.755	94.960	29.755
MIII(01)b-	29.766	94.989	29.766
MIII(01)b-	29.758	95.013	29.758
MIII(01)b-	29.742	95.065	29.742
MIII(01)b-	29.740	95.086	29.740
MIII(01)b-	29.747	95.092	29.747
MIII(01)b-	29.739	95.109	29.739
MIII(01)b-	29.758	95.158	29.758
MIII(01)b-	29.758	95.158	29.758
MIII(01)b-	29.759	95.178	29.759
MIII(01)b-	29.766	95.209	29.766
MIII(01)b-	29.766	95.209	29.766
MIII(01)b-	29.752	95.226	29.752
MIII(01)b-	29.768	95.264	29.768
MIII(01)b-	29.771	95.277	29.771
MIII(01)b-	29.778	95.298	29.778





MIII(01)b-:	29.858	95.199	29.858
MIII(01)b-:	29.858	95.199	29.858
MIII(01)b-:	29.799	95.229	29.799
MIII(01)b-:	29.946	95.089	29.946
MIII(01)b-:	30.016	95.028	30.016
MIII(01)b-:	29.946	95.089	29.946
MIII(01)b-:	29.957	95.082	29.957
MIII(01)b-:	29.920	95.105	29.920
MIII(01)b-:	29.890	95.147	29.890
MIII(01)b-:	29.890	95.147	29.890
MIII(01)b-:	29.754	95.045	29.754
MIII(01)b-:	29.758	95.013	29.758
MIII(01)b-:	29.738	95.983	29.738
MIII(01)b-:	29.848	95.701	29.848
MIII(01)b-:	29.738	95.983	29.738
MIII(01)b-:	29.844	95.703	29.844
MIII(00)b-	29.814	95.405	29.814
MIII(00)b-	29.887	95.447	29.887
M(00)Gs-1	29.506	94.899	29.506
M(00)b-22	29.488	94.947	29.488
M(00)b-24	29.488	94.947	29.488
M(00)b-39	29.475	94.979	29.475
M(00)b-59	29.429	94.049	29.429
M(00)b-67	29.352	95.153	29.352
M(00)b-76	29.309	95.177	29.309
M(00)b-77	29.309	95.177	29.309
M(00)Gs-1	29.399	94.628	29.399
M(01)b-2	29.526	94.881	29.526
M(01)b-13i	29.254	94.531	29.254
M(01)b-14i	29.254	94.531	29.254
366	29.721	92.619	29.721
370	29.620	95.480	29.620
372	29.591	95.469	29.591
373	29.543	95.455	29.543
376	29.525	95.454	29.525
380	29.743	95.712	29.743
382	29.742	95.692	29.742
385	29.710	95.578	29.710
b-18	29.002	95.521	29.002
b-10	29.306	95.643	29.306
b-35	29.320	95.345	29.320
b-45	29.454	95.419	29.454
b-88	29.389	95.369	29.389
b-98	29.683	94.541	29.683
b-76	29.627	94.629	29.627
b-9	29.610	94.652	29.610
b-143	29.602	95.606	29.602
BL-01-03	29.690	94.389	29.690
BL-02-03	29.811	94.422	29.811
BL-03-03	30.133	93.625	30.133
BL-04-03	30.032	93.636	30.032
BL-05-03	29.504	94.222	29.504
BL-06-03	29.504	94.260	29.504
BL-07-03	29.503	94.275	29.503
BL-08-03	29.491	94.316	29.491
BL-09-03	29.527	94.430	29.527
BL-10-03	29.207	94.548	29.207
BL-11-03	29.472	94.534	29.472
BL-12-03	29.450	94.515	29.450
BL-13-03	29.455	94.503	29.455
BL-14-03	29.457	94.486	29.457
BL-15-03	29.461	94.477	29.461
BL-16-03	29.464	94.450	29.464
BL-17-03	29.493	94.449	29.493
BL-18-03	29.520	94.451	29.520
GP-01-03	29.909	94.891	29.909
GP-02-03	29.909	94.891	29.909
GP-03-03	29.909	94.891	29.909
GP-04-03	29.909	94.891	29.909
GP-05-03	29.909	94.891	29.909
GP-06-03	29.909	94.891	29.909
GP-07-03	29.909	94.891	29.909
GP-08-03	29.909	94.891	29.909
GP-09-03	29.911	94.896	29.911
GP-10-03	29.923	94.884	29.923
GP-11-03	29.923	94.884	29.923
GP-12-03	29.923	94.884	29.923
GP-13-03	29.923	94.884	29.923
GP-14-03	29.923	94.884	29.923
GP-15-03	29.923	94.884	29.923
GP-16-03	29.934	94.902	29.934
GP-17-03	29.934	94.902	29.934
GP-18-03	29.874	94.906	29.874
GP-19-03	29.874	94.887	29.874
GP-20-03	29.884	94.888	29.884
GP-21-03	29.000	94.000	29.000
BT-01-03	30.057	95.032	30.057
BT-02-03	30.064	95.037	30.064
BT-03-03	30.066	95.039	30.066
BT-04-03	30.066	95.040	30.066
BT-05-03	30.072	95.049	30.072
BT-06-03	30.073	95.050	30.073
BT-07-03	30.073	95.050	30.073
BT-08-03	30.094	95.059	30.094
BT-09-03	30.044	95.029	30.044
BT-10-03	29.966	94.856	29.966
BT-11-03	29.961	94.843	29.961
BT-12-03	29.932	94.815	29.932
BT-13-03	29.942	94.813	29.942
BT-14-03	29.995	94.668	29.995
BT-15-03	29.996	94.668	29.996
BT-16-03	29.997	94.675	29.997
DX-01-03	30.027	94.630	30.027
TJ-01-03	30.801	92.600	30.801
NBK-01-23	29.694	92.239	29.694
NBK-02-23	29.694	92.239	29.694
NBK-03-23	29.694	92.239	29.694
NBK-04-23	29.694	92.239	29.694
NBK-05-23	29.121	94.231	29.121
NBK-06-23	29.188	94.196	29.188
NBK-07-23	29.188	94.196	29.188
NBK-08-23	29.279	94.315	29.279
NBK-08-23	29.311	94.464	29.311
NBK-09-23	29.254	94.454	29.254
NBK-10-23	29.254	94.454	29.254
NBK-11-23	29.288	94.463	29.288
NBK-12-23	29.288	94.463	29.288
NBK-13-23	29.339	94.415	29.339
NBK-14-23	29.339	94.415	29.339
NBK-15-23	29.439	94.691	29.439
NBK-16-23	29.242	94.262	29.242
NBK-17-23	29.242	94.262	29.242
NBK-18-23	29.443	94.704	29.443
NBK-19-23	29.443	94.704	29.443
NBK-20-23	29.446	94.728	29.446
NBK-21-23	29.460	94.750	29.460
NBK-22-23	29.521	94.872	29.521
NBK-23-23	29.521	94.872	29.521
NBK-24-23	29.521	94.872	29.521

NBK-25-23	29.522	94.878	29.522
NBK-26-23	29.660	94.917	29.660
NBK-27-23	29.660	94.917	29.660
NBK-28-23	29.567	94.908	29.567
NBK-29-23	29.567	94.908	29.567
NBK-30-23	29.567	94.908	29.567
NBK-31-23	29.567	94.908	29.567
NBK-32-23	29.567	94.908	29.567
NBK-33-23	29.537	94.894	29.537
NBK-34-23	29.488	94.831	29.488
NBK-35-23	29.488	94.831	29.488
NBK-36-23	29.488	94.831	29.488
NBK-37-23	29.489	94.945	29.489
NBK-38-23	29.488	94.934	29.488
NBK-39-23	29.885	94.899	29.885
NBK-40-23	29.895	94.902	29.895
NBK-41-23	30.241	95.770	30.241
NBK-42-23	29.756	95.705	29.756
NBK-43-23	29.760	95.705	29.760
NBK-44-23	29.761	95.701	29.761
NBK-45-23	29.657	94.725	29.657
NBS-101-2	29.168	93.517	29.168











**Table DR4+5****Methods, Apatite and Zircon U-Th/He Analysis**

$^4\text{He}$  and  $^3\text{He}$  were measured using a Balzers bakeable quadrupole mass spectrometer designed for UHV operation, fitted with both Faraday and electron multiplier detectors. Under typical operating conditions using the multiplier the system has an effective sensitivity of 1000 amps/mole. For He extractions, we use a double-vacuum resistance furnace. An all-metal sample dropper designed around a linear-motion feedthrough permitted multiple samples to be loaded for sequential analysis in the resistance furnace. Helium evolved from heated samples was purified in an all-metal extraction line pumped by a Varian ion pump during routine operation as well as a 70 l/s turbomolecular pump and a small rotary backing pump during bakeout. Getting of active gases was handled by a SAES getter in the extraction line; a smaller SAES getter in the mass spectrometer volume was used to lower hydrogen peaks. Reservoirs containing a  $^3\text{He}$  spike and a  $^4\text{He}/^3\text{He}$  standard are attached to the line behind all-metal pipettes. Two temperature-stabilized capacitance manometers provide precise, accurate pressure measurements used for spike preparation. The extraction line  $^4\text{He}$  blank is  $1 \times 10^{-16}$  moles or less. Th and U values were measured by D. Peter Reiners lab at Yale University and later the University of Arizona, using isotope-dilution analysis; apatites underwent a nitric-acid digestion and zircons a hydrofluoric acid treatment in pressure vessels. U and Th analysis was done on the same grains from which He was extracted.

$^4\text{He}$  was measured in two ways: by isotope dilution using a  $^3\text{He}$  spike and manometrically by comparison to calibration shots run before, during and after each sample batch. In addition to the  $^3\text{He}$  spike used for routine isotope-dilution measurements, a mixed  $^4\text{He}/^3\text{He}$  standard is used to determine and monitor mass discrimination and to build the daily manometric calibration. Over short to medium-term periods spanning the analysis of several sample batches, we found the  $^4\text{He}/^3\text{He}$  ratio for the calibration standard to be precise to within 0.3%, with a value of about 0.800 (the true  $^4\text{He}/^3\text{He}$  ratio of our standard is 1.000). The size of a typical spike was  $4.8 \times 10^{-13}$  moles. While in theory there are many advantages to the isotope-dilution approach, we found in practice that spike and manometric determinations tended to agree within 1%. Further, because our system is not fitted with a cryotrap, hydrogen loads can be a problem despite gettering, and we noted that when the spike and manometric calibrations disagreed in nearly every case the disagreement correlated with the presence of a high hydrogen load. We suspect this leads to a small mass interference at  $m/e=3$ , an overestimate in the size of the  $^3\text{He}$  beam, and a consequent underestimate of the  $^4\text{He}$  signal from the unknown. Thus, the data we report are all based on the manometric calibration.

When these samples were run early in the history of the lab, most samples were run in duplicate although in a number of cases and for later analyses, triplicates were run, especially for apatite. Generally for zircons 1-2 grains were analyzed per aliquot, and 3-4 but sometimes up to 8 for apatites. For both apatites and zircons, we picked unbroken, symmetric grains without visible inclusions under a high-power binocular microscope. Samples were digitally photographed in order to record their dimensions for calculation of alpha-correction factors. Apatites were placed in small Pt (and later Nb) tubes whose ends are crimped. Zircons were placed in first very small handmade Nb-foil packets and for later samples, small Nb tubes. In order to transfer samples with the dropping mechanism and identify samples after retrieval from the furnace, grain-containing packets and tubelets were placed in scribed Pt or Nb-foil carrier packets.



Samples are loaded into the dropping mechanism so that those with lower estimated helium contents are analyzed first. After a brief overnight bake at 70 to 100°C and high-temperature outgassing of the empty crucible to lower hydrogen pressures, samples are outgassed sequentially. Earlier apatite samples were heated to 950 °C for 15 minutes, but although diffusion theory predicts this temperature to be more than sufficient, not infrequently we found incomplete outgassing that left a few percent of a refractory component behind. Heating to 1100°C for 15 minutes appeared sufficient to completely outgas apatites, and most samples were run under these conditions. Similarly for zircons, 1150° C of heating for 15 minutes should suffice, but we found it necessary to heat samples for 1350°C for 60 minutes to consistently and completely outgas zircons to blank levels. For our earlier samples re-extract analyses were run frequently to check for complete outgassing; this was done less often as we gained experience that the higher-temperature heating was working. Following heating, sample gas was expanded and circulated over the main getter. The spike was then added, and the gas introduced to the mass spectrometer. All gas transfers were by progressive expansion, not cryotrapping. Masses 2, 3, and 4 were measured using software belonging to the quadrupole, and then time-zero beams and uncertainties were determined using a house-built LabVIEW regression module before final spreadsheet-based data reduction

Over the time that our reported data were obtained we obtained a mean age of  $32.00 \pm 0.18$  (1 standard error, n=50) for the Durango apatite standard (for internal shards). For this standard, McDowell et al. (2005) reported a direct U-Th/He age of  $31.13 \pm 0.21$  (1 S.E.) and an Ar-Ar age of  $31.44 \pm 0.22$ (1 S.E.). For Fish Canyon zircon, for which Schmitz and Bowring (2001) reported a precise U-Pb age of  $28.476 \pm 0.015$  (1 S.E), over the sample time interval we obtained a mean U-Th/He age of  $28.43 \pm 0.35$  (1 S.E., n=26). The larger scatter in the zircon data is probably due to the greater U and Th zoning seen in zircon compared to apatite plus the need to make a correction for alpha ejection in the discrete zircon grains.

For these samples measured in the earlier days of the laboratory, alpha-ejection corrections were calculated for appropriate grain shapes (sphere, cylinder or tetragonal, oblate spheroid) and 2D data (length and width), using the methods of Farley et al. (1996) with alpha-recoil distances summarized in Ketcham (2005).





















LU1380-005	840 °C	1,788.0	-	105,047.1	324,566	1,275,026	13.71	0.21	70.38	10.88
LU1380-006	920 °C	2,292.6	-	100,698.9	305,926	1,186,157	13.53	0.17	63.38	10.25
LU1380-007	1000 °C	3,565.0	-	160,746.6	477,350	1,970,138	14.40	0.16	64.89	16.00
LU1380-008	1050 °C	1,478.7	-	186,091.7	573,938	2,311,548	14.06	0.09	83.65	19.24
LU1380-009	1090 °C	690.2	-	136,940.0	431,362	1,717,803	13.90	0.12	88.87	14.46
LU1380-010	1130 °C	439.6	-	90,435.4	293,342	1,157,587	13.77	0.08	89.39	9.83
LU1380-011	1160 °C	237.4	-	41,908.5	137,234	554,896	14.11	0.09	88.28	4.60
LU1380-012	1200 °C	91.1	-	22,055.5	74,941	380,709	17.71	0.15	92.96	2.51
LU1380-013	1300 °C	131.4	-	3,716.7	21,665	246,475	39.42	0.58	86.22	0.73

#### Biotite Total-Fusion Analyses

Lab Number-Step	Temperature	<sup>36</sup> Ar (cps)	<sup>37</sup> Ar <sub>Ca</sub> (cps)	<sup>38</sup> Ar <sub>Cl</sub> (cps)	<sup>39</sup> Ar <sub>K</sub> (cps)	<sup>40</sup> Ar* (cps)	Age (Ma)	Error (Ma 2σ)	<sup>40</sup> Ar* (%)	<sup>39</sup> Ar <sub>K</sub> (%)
<i>IG-4, J = 0.00038349</i>										
LU1461-001	laser fusion	3,440.6	-	40,417.0	108,154	300,360	1.92	0.21	22.76	7.37
<i>BT20E-02, J = 0.00038282</i>										
LU1462-001	laser fusion	1,060.2	-	565.1	13,478	832,781	42.35	1.29	72.64	0.92
<i>BT-21E-02, J = 0.00038241</i>										
LU1463-001	laser fusion	1,929.3	-	2,844.5	49,273	1,495,015	20.92	0.72	72.35	3.36
<i>b-289, J = 0.00037882</i>										
LU1469-001	laser fusion	1,631.2	-	83.4	55,606	18,719	0.23	0.14	3.73	3.79
<i>b-278, J = 0.00037822</i>										
LU1470-001	laser fusion	5,211.0	-	3,201.4	58,498	37,497	0.44	0.54	2.37	3.99
<i>b-39, J = 0.00037686</i>										
LU1472-001	laser fusion	2,024.1	-	22,686.9	103,922	668,803	4.46	0.24	52.68	7.09
<i>BL-11-03, J = 0.00037585</i>										
LU1475-001	laser fusion	24,817.3	-	1,755.2	35,922	663,413	12.76	3.02	8.29	2.45
<i>BL-13-03, J = 0.00037545</i>										
LU1479-001	laser fusion	313.4	-	1,417.3	31,656	279,728	6.12	0.19	74.97	2.16
<i>BT-02-03, J = 0.00037526</i>										
LU1480-001	laser fusion	2,080.1	-	21,245.9	132,529	717,264	3.75	0.17	53.72	9.04
<i>BT-12-03, J = 0.00037482</i>										
LU1482-001	laser fusion	1,511.1	-	3,269.8	74,689	1,736,006	16.05	0.52	79.47	5.09
<i>BT-13-03, J = 0.00037467</i>										
LU1483-001	laser fusion	3,149.4	-	6,128.2	98,311	2,906,909	20.39	0.65	75.70	6.70
<i>NBK-83B-25, J = 0.00037408</i>										
LU1485-001	laser fusion	2,744.1	-	49,972.5	150,939	616,117	2.83	0.12	43.06	10.29
<i>NB-01-26, J = 0.00037400</i>										
LU1486-001	laser fusion	4,852.5	-	12,390.0	125,057	1,691,792	9.36	0.37	54.07	8.53
<i>NB-05-26, J = 0.00037385</i>										
LU1487-001	laser fusion	1,584.5	-	751.1	38,238	5,074,446	89.76	2.70	91.54	2.61
<i>NB-07-26, J = 0.00037377</i>										
LU1488-001	laser fusion	1,719.6	-	1,776.8	47,210	3,953,791	57.16	1.76	88.59	3.22
<i>NB-13-26, J = 0.00037358</i>										
LU1489-001	laser fusion	2,282.2	-	48,561.6	201,302	3,183,213	10.93	0.33	82.42	13.73
<i>NB-10-26, J = 0.00037354</i>										
LU1490-001	laser fusion	2,328.1	-	5,439.7	141,898	2,010,125	9.80	0.32	74.40	9.67

#### Notes:

- (1) Argon-isotope abundances in volts or counts per second, corrected for blank, mass discrimination, and as appropriate, decay following irradiation and nucleogenic interferences
- (2) Age for GA 1550 monitor used to determine J-values: 98.79 Ma.
- (3) For samples run using ion counting, <sup>37</sup>Ar not measured due to long delay following irradiation; this should not be significant given the high K/Ca of biotite
- (4) Uncertainties are two-sigma.

## Table DR6

### Methods, $^{40}\text{Ar}/^{39}\text{Ar}$ Analysis

$^{40}\text{Ar}/^{39}\text{Ar}$  dating employed an automated furnace and laser extraction systems connected on-line to a VG 3600 noble-gas mass spectrometer. The furnace line is built around a double-vacuum resistance furnace utilizing Mo crucibles. Furnace temperature is monitored by a W-Re thermocouple. Temperature precision within the normal working range 400-1600°C is typically  $\pm 1^\circ\text{C}$ , with small temperature gradients of less than 2-3°C. The vacuum in the furnace outer jacket is maintained by a 60 l/s turbomolecular pump, while the extraction line itself is pumped by a 30 l/s ion pump. Sample cleanup is provided by two SAES internally heated getter pumps and optionally by a cold finger cooled to LN<sub>2</sub> temperature. Blanks of  $<1.5 \times 10^{-15}$  moles of  $^{40}\text{Ar}$  at 1200°C are routinely achieved in the furnace line after several days of pumping time. The laser extraction line is equipped with a Merchantek dual CO<sub>2</sub>/UV laser system. Most of our routine laser work is performed with the CO<sub>2</sub> laser, which produces a continuous 10.6  $\mu\text{m}$  beam with output power variable up to 35 W. The laser sample chamber accepts copper trays holding up to 200 samples each and is positioned by a Newport 3-axis motion control system operable under computer control. Gas cleanup in the laser line is handled by SAES getters; for larger hydrous samples, a LN<sub>2</sub>-cooled cold finger is available. All valves essential for gas handling on both extraction systems can be operated under computer control. Blanks for the laser line (5 min. static vacuum) are typically  $<4 \times 10^{-16}$  moles of  $^{40}\text{Ar}$ .

The VG 3600 mass spectrometer was operated at 4.5 kV accelerating potential and 100 mA trap current. Under these conditions the background for  $^{36}\text{Ar}$  is  $1 \times 10^{-14}$  cc STP; on-line to the furnace extraction system the effective sensitivity is  $4.8 \times 10^{-15}$  moles/mV using the faraday detector. Argon analyses were performed using an ion-counting electron multiplier. The ion-counting system has a dead time of 25 ns and an effective sensitivity of  $\sim 1.2 \times 10^{-19}$  moles/cps open to the furnace line. During routine analyses, the five Ar peaks and associated baselines were measured repeatedly over 7-10 measurement cycles. Typical counting times were 4 seconds for large peaks, and 10 seconds for small peaks and baselines. Our measurements of atmospheric argon typically yielded  $^{40}\text{Ar}/^{36}\text{Ar}$  values of about 285 to 290 with a precision of about 0.75%. The mass spectrometer and extraction lines are integrated into a fully automated system under the control of a PC running LabSpec, a LabVIEW program for noble-gas mass spectrometry developed at Lehigh by Dr. Bruce Idleman.

Sample irradiation was carried out in the McMaster reactor in Hamilton, Ontario. Most irradiations were performed unshielded. Prior to irradiation, following conventional mineral separation samples were handpicked to remove any impurities and then washed repeatedly in deionized water and ethanol before packaging in aluminum or copper foil. Flux monitors were interspersed both vertically and laterally within the irradiation package. Interferences from Ca and K were monitored by analyzing CaF<sub>2</sub> and K<sub>2</sub>SO<sub>4</sub> included with every irradiation.

Raw data from the mass spectrometer was reduced using ArArCalc, an Excel add-on written by Anthony Koppers. Beam values are regressed to time of inlet to the mass spectrometer, then corrected for background, line blank, discrimination, decay of  $^{37}\text{Ar}$  and  $^{39}\text{Ar}$ , and Ca and K-derived nucleogenic interferences. Typical analytical precision for single-crystal laser-fusion analyses of biotite age standard GA-1550 (98.5 Ma; Spell and McDougall, 2003) is  $\sim 0.3\%$ . GA-1550 biotite was used as the irradiation standard.

We analyzed most biotites with an abbreviated step-heating schedule because in our experience whether measured biotite ages make geological sense or not cannot be predicted from the shape or quality of their age spectra, which usually are flat and if not, can be explained by inclusions, or alteration and weathering. The step-heating results do have the advantage of allowing internal isochrons to be used to test the assumption of whether the trapped argon in a sample is atmospheric in composition or not. Because of time pressure and lab difficulties, one suite of biotites were simply run as total-fusion analyses.



## Table DR7b. BT-33-02 K-feldspar: Inversion information and parameters

Parameters used to run the code Arvert 4.1

### Model 1 – Monotonic cooling only

```
SAMPLE INFO:    LU1225 BT33 Kspar
FILE SUFFIX:   bt33finmhf

CRS ITERATIONS: 15000
MODEL DURATION (m.y.): 30.0
TIME NODES:    15
CONSTRAINING BRACKETS tT: 4
TIME          TMIN      TMAX
30.0         450.0     500.0
28.0         250.0     500.0
20.0         250.0     500.0
0.0          0.0       500.0
MAX MONTE-CARLO HEATING RATE: 5.0
MAX MONTE-CARLO COOLING RATE: 60.0
MAX CRS HEATING RATE: 0.0
MAX CRS COOLING RATE: 500.0
CRS AMPLIFICATION FACTOR: 1.50
SUBSET SIZE, POOL SIZE: 15 150
FITTING CRITERION: 1.00
FITTING OPTION: 1 (mean percent)
DIFFUSION GEOMETRY: 2 (infinite-slab)
RESTART OPTION: 0 (new start from Monte-Carlo
histories)
DISCRETIZATION DELTA-TEMPERATURE: 1.0
LOVERA SERIES CUT-OFF: 1.0e-05
FLAG TO WRITE FULL REPORTS: 1
```

```
***** Mineral-Age Info *****
IS MINERAL AGE A CONSTRAINT?: 0 - no
```

#### DOMAIN INFO

-----  
Domains: 5

	E	D0	frac.
1	48.79	4.73156e+21	0.104
2	48.79	3.21739e+20	0.150
3	48.79	1.19317e+19	0.082
4	48.79	5.56165e+17	0.235
5	48.79	1.40057e+16	0.428

#### Goal Age Spectrum

-----  
Goal spectrum steps: 61

	f39	age	error	skip?
1	0.003	432.5	19.6	0
2	0.004	43.6	4.2	0
3	0.008	19.3	1.3	0
4	0.010	11.5	1.7	0
5	0.014	10.0	1.1	0
6	0.017	6.8	1.5	0
7	0.023	6.6	0.7	0
8	0.028	4.9	0.8	0
9	0.036	4.4	0.5	0
10	0.043	3.4	0.7	0
11	0.057	3.6	0.3	0
12	0.067	3.1	0.4	0
13	0.082	3.0	0.3	0
14	0.093	2.6	0.4	0
15	0.115	2.8	0.2	0
16	0.130	2.4	0.3	0
17	0.155	2.4	0.2	0
18	0.172	2.3	0.3	0
19	0.196	2.4	0.2	0
20	0.213	2.1	0.3	1
21	0.235	2.4	0.2	0
22	0.250	2.2	0.3	1
23	0.269	2.6	0.2	0
24	0.282	2.4	0.4	1
25	0.298	2.7	0.3	1
26	0.316	2.9	0.3	1
27	0.334	2.9	0.3	1
28	0.357	4.4	0.2	1
29	0.380	4.5	0.2	1
30	0.406	5.9	0.2	1
31	0.435	7.5	0.2	1
32	0.468	9.1	0.2	1
33	0.501	9.8	0.2	1
34	0.533	10.5	0.2	1
35	0.565	10.8	0.2	1
36	0.586	10.5	0.2	1
37	0.603	10.8	0.3	1
38	0.637	10.9	0.2	1
39	0.659	11.5	0.2	1
40	0.677	12.5	0.3	1
41	0.691	12.6	0.3	1
42	0.721	13.3	0.4	1
43	0.744	13.4	0.4	1
44	0.761	13.8	0.4	0
45	0.776	13.5	0.5	0
46	0.789	13.6	0.7	0
47	0.800	14.5	0.7	0
48	0.810	13.7	0.7	0
49	0.819	13.3	0.8	0
50	0.825	13.8	1.0	0
51	0.826	14.1	4.2	0



52	0.828	14.1	2.1	0
53	0.832	14.9	1.2	0
54	0.840	15.3	0.6	0
55	0.854	15.9	0.3	0
56	0.865	14.8	0.4	0
57	0.902	15.4	0.2	0
58	0.947	13.4	0.2	0
59	0.973	11.0	0.2	0
60	0.986	10.0	0.4	0
61	0.998	11.4	0.4	0

\*\*\*\*\* Arvert 4.1.0 finished with no worries! \*\*\*\*\*

Processed 15000 CRS histories  
in 7.58 minutes at a rate of 0.051 minutes per 100 histories

Best fit is 6.11, worst fit is 7.69

**Model 2 – Reheating at modest rates permitted cooling only**

```

SAMPLE INFO: LU1225 BT33 Kspar
FILE SUFFIX: bt33finhhf

CRS ITERATIONS: 15000
MODEL DURATION (m.y.): 30.0
TIME NODES: 15
CONSTRAINING BRACKETS tT: 4
TIME TMIN TMAX
30.0 450.0 500.0
28.0 250.0 500.0
20.0 250.0 500.0
0.0 0.0 500.0
MAX MONTE-CARLO HEATING RATE: 5.0
MAX MONTE-CARLO COOLING RATE: 60.0
MAX CRS HEATING RATE: 10.0
MAX CRS COOLING RATE: 500.0
CRS AMPLIFICATION FACTOR: 1.50
SUBSET SIZE, POOL SIZE: 15 150
FITTING CRITERION: 1.00
FITTING OPTION: 1 (mean percent)
DIFFUSION GEOMETRY: 2 (infinite-slab)
RESTART OPTION: 0 (new start from Monte-Carlo
histories)
DISCRETIZATION DELTA-TEMPERATURE: 1.0
LOVERA SERIES CUT-OFF: 1.0e-05
FLAG TO WRITE FULL REPORTS: 1

***** Mineral-Age Info *****
IS MINERAL AGE A CONSTRAINT?: 0 - no

```

DOMAIN INFO

-----  
 Domains: 5

	E	D0	frac.
1	48.79	4.73156e+21	0.104
2	48.79	3.21739e+20	0.150
3	48.79	1.19317e+19	0.082
4	48.79	5.56165e+17	0.235
5	48.79	1.40057e+16	0.428

Goal Age Spectrum

-----

Goal spectrum steps: 61

	f39	age	error	skip?
1	0.003	432.5	19.6	0
2	0.004	43.6	4.2	0
3	0.008	19.3	1.3	0
4	0.010	11.5	1.7	0
5	0.014	10.0	1.1	0
6	0.017	6.8	1.5	0
7	0.023	6.6	0.7	0
8	0.028	4.9	0.8	0
9	0.036	4.4	0.5	0
10	0.043	3.4	0.7	0
11	0.057	3.6	0.3	0
12	0.067	3.1	0.4	0
13	0.082	3.0	0.3	0
14	0.093	2.6	0.4	0
15	0.115	2.8	0.2	0
16	0.130	2.4	0.3	0
17	0.155	2.4	0.2	0
18	0.172	2.3	0.3	0
19	0.196	2.4	0.2	0
20	0.213	2.1	0.3	1
21	0.235	2.4	0.2	0
22	0.250	2.2	0.3	1
23	0.269	2.6	0.2	0
24	0.282	2.4	0.4	1
25	0.298	2.7	0.3	1
26	0.316	2.9	0.3	1
27	0.334	2.9	0.3	1
28	0.357	4.4	0.2	1
29	0.380	4.5	0.2	1
30	0.406	5.9	0.2	1
31	0.435	7.5	0.2	1
32	0.468	9.1	0.2	1
33	0.501	9.8	0.2	1
34	0.533	10.5	0.2	1
35	0.565	10.8	0.2	1
36	0.586	10.5	0.2	1
37	0.603	10.8	0.3	1
38	0.637	10.9	0.2	1

39	0.659	11.5	0.2	1
40	0.677	12.5	0.3	1
41	0.691	12.6	0.3	1
42	0.721	13.3	0.4	1
43	0.744	13.4	0.4	1
44	0.761	13.8	0.4	0
45	0.776	13.5	0.5	0
46	0.789	13.6	0.7	0
47	0.800	14.5	0.7	0
48	0.810	13.7	0.7	0
49	0.819	13.3	0.8	0
50	0.825	13.8	1.0	0
51	0.826	14.1	4.2	0
52	0.828	14.1	2.1	0
53	0.832	14.9	1.2	0
54	0.840	15.3	0.6	0
55	0.854	15.9	0.3	0
56	0.865	14.8	0.4	0
57	0.902	15.4	0.2	0
58	0.947	13.4	0.2	0
59	0.973	11.0	0.2	0
60	0.986	10.0	0.4	0
61	0.998	11.4	0.4	0

\*\*\*\*\* Arvert 4.1.0 finished with no worries! \*\*\*\*\*

Processed 15000 CRS histories  
in 8.47 minutes at a rate of 0.056 minutes per 100 histories

Best fit is 3.64, worst fit is 3.94

## **Table DR8 - Parameters used in thermal modeling**

We used the Pecube finite-element model, version 1 (Braun, 2003) to investigate the importance of lateral heat flow away from the rapidly advected rocks within the Namche Barwa massif.

### Crustal parameters used in model, and comments:

- no heat production (given that the goal of the modeling was to look at lateral heat flow in the shallow to mid crust, and given that heat production values are poorly constrained in magnitude and distribution, we removed this parameter from consideration);
  - thermal diffusivity of  $31.6 \text{ km}^2/\text{m.y.}$  (not temperature-dependent);
  - temperature at the model base of  $840^\circ\text{C}$ ;
  - fixed surface topography that is the mean for a swath perpendicular to the seismically active zone.
- 
- Together with a mean model thickness of 40 km (from base up to mean elevation), these parameters yield an average starting geotherm of about  $20^\circ\text{C}/\text{km}$ , a reasonable value for a plutonic arc of this age (Rothstein and Manning, 2003).
  - Given that the substantial exhumation involved in these model runs was greater than the model thickness, the closest natural analog for this model would be the lateral flow of mid or lower-crustal material into the massif that is then diverted upward and eroded from a steady-state landscape.

The basic Pecube code was modified to place a vertical fault in the model that could be activated some time after start of the model run. This fault was placed at the basement-cover contact at a distance of 16 km into the model space (see Figure 11 in the main text). Runs were essentially 2.5D, as the modeled block simply had the same topographic profile used along the profile-parallel direction. Models were 80 km in length and width, leaving 64 km of half-space into which to diffuse heat without interfering with the lateral no-flow boundary condition. The model had 321 nodes in the important profile-parallel direction, 11 nodes in the unimportant cross-profile direction and 101 vertical nodes.

Each model was first run for 5 m.y. at a  $0.25 \text{ mm/yr}$  exhumation rate, to equilibrate isotherms beneath the topography. After that time, rapid exhumation was turned on within the massif for varying durations and exhumation rates. Figure 19 in the main text shows results for two plausible combinations of parameters: extremely rapid exhumation at  $10 \text{ mm/yr}$  for 5 m.y. duration, and rapid exhumation at  $5 \text{ mm/yr}$  for 10.y. duration (both combinations involve total exhumation of 50 km).